
EUROPEAN of Molecular Journal **Biotechnology**

Has been issued since 2013.
E-ISSN 2409-1332
2021. 9(1). Issued once a year

EDITORIAL BOARD

Novochadov Valerii – Volgograd State University, Russian Federation (Editor in Chief)
Goncharova Nadezhda – Research Institute of Medical Primatology, Sochi, Russian Federation
Garbuzova Victoriia – Sumy State University, Ukraine
Ignatov Ignat – Scientific Research Center of Medical Biophysics, Sofia, Bulgaria
Malcevschi Alessio – University of Parma, Italy
Nefedeva Elena – Volgograd State Technological University, Russian Federation
Kestutis Baltakys – Kaunas University of Technology, Lithuania
Tarantseva Klara – Penza State Technological University, Russian Federation
Venkappa S. Mantur – USM-KLE International Medical College, Karnatak, India

Journal is indexed by: **Chemical Abstracts Service** (USA), **CiteFactor** – Directory of International Research Journals (Canada), **Cross Ref** (UK), **EBSCOhost Electronic Journals Service** (USA), **Global Impact Factor** (Australia), **Journal Index** (USA), **Electronic scientific library** (Russian Federation), **Open Academic Journals Index** (USA), **Sherpa Romeo** (Spain), **ULRICH's WEB** (USA).

All manuscripts are peer reviewed by experts in the respective field. Authors of the manuscripts bear responsibility for their content, credibility and reliability.

Editorial board doesn't expect the manuscripts' authors to always agree with its opinion.

Postal Address: 1367/4, Stara Vajnorska str., Bratislava – Nove Mesto, Slovakia, 831 04
Release date 15.09.21
Format 21 × 29,7/4.

Website: <http://ejournal8.com/>
E-mail: aphr.sro@gmail.com
Headset Georgia.

Founder and Editor: Academic Publishing House Researcher s.r.o.
Order № 22.

European Journal of Molecular Biotechnology

2021

Is. **1**

CONTENTS

Articles

Features of Glucose Utilization and Oxygen Consumption by Mcf-7 Breast Cancer Cells Depending On in Vitro Culture Conditions A.H. Al-Humairi, O.V. Ostrovskiy, E.V. Zykova, D.L. Speransky, V.V. Udut, M.A. Buldakov	3
Antimicrobial and Dyeing Studies of Some Novel Reactive Mono(bis mono), Tri(bis tri) Methine Cyanine Dyes based on Cyano Pyridazine Nucleus M.M. Gomaa, S.A. Mahmoud	12
Ligand and ASIC Receptor Interactions in a Rat Ischemic Stroke Model E.N. Nesmeyanova, G.A. Sroslova, M.V. Postnova, N.V. Panin, Yu.A. Zimina	26
Evaluation of Protective Potential of Ethyl Acetate Extract of Cocus Nucifera in Gentamycin Induced Nephrotoxicity in Albino Mice I. Nathaniel Onuche, A. Joseph Oluwatope	31
Insight into the Natural and Synthetic Factors Responsible for Cell Regeneration in Various Organs S. Mukherjee, S. Das, S. Kumari Rowlo, A. Pk	37

Copyright © 2021 by Academic Publishing House Researcher s.r.o.



Published in the Slovak Republic
European Journal of Molecular Biotechnology
Has been issued since 2013.
E-ISSN: 2409-1332
2021. 9(1): 3-11

DOI: 10.13187/ejmb.2021.1.3
www.ejournal8.com



Articles

Features of Glucose Utilization and Oxygen Consumption by MCF-7 Breast Cancer Cells Depending On *in vitro* Culture Conditions

Ahmed H. Al-Humairi ^{a, b, *}, Oleg V. Ostrovskiy ^a, Ekaterina V. Zykova ^a, Dmitriy L. Speransky ^a, Vladimir V. Udut ^c, Mikhail A. Buldakov ^d

^a Volgograd State Medical University, Russian Federation

^b University of Babylon, Iraq

^c Goldberg Research Institute of Pharmacology and Regenerative Medicine, Tomsk National Medical Research Center of Russian Academy of Sciences, Russian Federation

^d Cancer Research Institute, Tomsk National Medical Research Center of Russian Academy of Sciences, Russian Federation

Abstract

This study aimed to show the possibility of regulating the metabolic capabilities of cancer cells *in vitro* by changing the medium composition, using the MSF-7 breast cancer cell line as an example. The relevance of the work is due to the solid necessity for constantly improve cell lines for testing new antitumor drugs and obtaining new information about the chemistry of cancer.

The assessment of glucose oxidation type by measuring the production of lactate and polarographic determination of oxygen consumption under normal conditions and the influence of Oligomycin A, 2,4 Dinitrophenol, or Rotenone action were basic methods of this study. An excess of glucose or removing glutamine was created as medium composition changes. A culture of Vero non-tumor cells was applied as a comparative model.

As a result, the lactate production by MCF-7 tumor cell culture is significantly higher than the same by Vero culture, which is consistent with the Warburg effect. Excess glucose led to decreased lactate production in MCF-7 culture by almost 10 %, but it was not observed for Vero culture. The glutamine decrease in the culture medium does not significantly affect the change in lactate production for both Vero cells and MCF-7 cells. In the culture of tumor cells, excess glucose and lack of glutamine during daily incubation did not statistically affect respiration, while these changes were accompanied by a decrease in oxygen consumption by cells by 10 % and 15 %, respectively, in the culture of Vero cells.

The obtained data can be used to control the cultivation system and verify metabolic changes due to testing new antitumor agents *in vitro*.

Keywords: breast cancer, cell lines, MSF-7 cells, Vero cells, cancer cell metabolism, glucose utilization, oxygen consumption.

* Corresponding author

E-mail addresses: ahmed.h.mneahil@gmail.com (A.H. Al-Humairi)

1. Introduction

Malignant neoplasms are one of the leading causes of death from diseases. According to the World Health Organization, about 8 million people die from cancer every year in the world. Breast cancer is one of the most dangerous types of cancer among women. The five-year survival rate of women diagnosed with metastatic breast cancer is slightly less than 30 % (Bray et al., 2018, DeSantis et al., 2016).

Even though many approaches are used for cancer treatment, including surgical and radiation ones, chemotherapy is one of the primary treatments at all stages of breast cancer in combined regimens. For metastatic cancer, chemotherapy becomes the method of choosing (O'Shaughnessy et al., 2012).

Since the disease is polymorphic, and chemotherapeutic agents necessarily pass the *in vitro* testing stage, we need to identify and study different human breast cancer cell lines constantly.

The most relevant is assessing the metabolic phenotype of tumor cells due to the widespread prevalence of oncological diseases and the emergence of new, more accurate, and powerful equipment (Clegg et al., 2020, Dai et al., 2017).

The tumor transformation of cells is a complex multi-stage process that leads to a change in many fundamental principles of metabolism. It is widely known that tumor cells acquire the ability to unlimited proliferation (1); growth autonomy and insensitivity to growth factors (2); metastasis progression (3); genome instability and metabolic reprogramming (4); and apoptosis avoidance (5). The metabolic reprogramming in a tumor cell affects all vital pathways as the exchange of proteins, fats, and carbohydrates, allowing transformed cells to adapt to new conditions of existence (Butler et al., 2020, El-Sahli, Wang, 2020, Kang et al., 2018).

Glucose is the primary source of energy in cells. Under normal conditions, aerobic glycolysis dominates in human cells, thanks to which glucose utilization formed 90 % ATP. During anaerobic glycolysis, pyruvate is converted into lactate, some of which is then converted into acetyl-CoA in the mitochondria and then is oxidized to CO₂ (Nelson, Cox, 2014).

Increased glucose uptake is typical for tumor cells. As a result, the increased lactate formation manifested in its early stages of tumor transformation even with high oxygen content in the medium. This change is called the Warburg effect, implemented at the expense of high intensity of anaerobic glycolysis. The active use of glutamine and the synthesis of higher fatty acids are other essential features of cancer cell metabolism (Gentric et al., 2017, Van der Heiden, DeBerardinis 2017).

These metabolic differences between normal and cancer cells can serve as a biochemical basis for developing new antitumor drugs. Inhibition of glycolysis, changes in glutamine metabolism, and fatty acid synthesis are three possible approaches to antitumor metabolic therapy (Bhardwaj, He, 2020, Park et al., 2020, Pattni et al., 2017). In practice, a combination of traditional chemotherapy with drugs that affect a particular stage of cancer cell metabolism is the most effective method of tumor therapy.

Based on the above, we have devoted this study to evaluate the features of glucose utilization and energy metabolism by tumor cells *in vitro* culture under when metabolic control by changing the culture medium composition.

2. Material and methods

Characteristics of tumor cell cultures

MCF-7 culture is one of the primary cell lines of human breast cancer, so we used it in this study. Currently, MCF-7 is the most popular line for studying the cytotoxicity of antitumor agents and for the molecular features of breast cancer. The MCF-7 cells have an epithelial-like structure, express estrogen receptors, and synthesize estradiol, making them optimal targets for studying receptors and chemotherapy. MCF-7 lines form monolayer cultures with a survival rate of up to 95 % and a confluence of up to 100 % due to the preservation of reproductive ability (Alexandrova et al., 2019, Comsa et al., 2015).

The transferable Vero culture is the renal epithelial cells of the African green monkey. It is widely used to cultivate viruses, detect Escherichia coli toxins, and host cells for eukaryotic parasites. The Vero cells have a fibroblast-like structure. They form monolayer cultures on media with a survival rate of 70-90 % and up to 100 % (Osada et al., 2014). In our work, we used the Vero cell line as a variant of non-tumor phenotypes for comparison with the behavior of the MCF-7 line.

Applied kits and reagents

Table 1 presents the list and purpose of the used kits and reagents by their application in this study.

Table 1. Characteristics of the kits and reagents applied in the study

Kit/Reagent	Application	Abbreviation
Medium MEM without glutamine (PanEco)	Cell culture	MEM
Medium DMEM without glutamine (PanEco)		DMEM
Fetal calf serum (PanEco)		FCS
2 mM solution of L-glutamine (PanEco)		Glutamine
6 mM solution of D-Glucose (PanEco)		Glucose
A mixture of antibiotics (streptomycin + penicillin, PanEco)		AB
Trypsin 0.25% solution (PanEco)		Trypsin
Versen's solution (PanEco)	Manipulations with cells	VS
Hanks' solution (PanEco)		HS
Buffer, pH 7.5, tris-HCl 50 mM, p-chlorophenol 6.0 mM (Sigma)		TrisB
Trypan blue solution (PanEco)		Determination of viability
70 % ethyl alcohol	Antiseptics	Eth
3.3 mM lactic acid solution (Sigma)	Lactate measuring	Lactat
Kit for lactate measuring of Olvex Diagnosticum		Olvex kit
Polarography medium (1 mM EDTA + 1.2 mM MgCl ₂ + 1 M taurine + 5 mM KH ₂ PO ₄ + 20 mM HEPES buffer + 100 mM sucrose, pH 7.4)	Polarography	PM
10 μM of Oligomycin A solution (Sigma-Aldrich)		Oligomycin
100 μM of 2,4-dinitrophenol solution (Sigma)		DNP
10 μM of Rotenone solution (Sigma-Aldrich)		Rotenone
3 M solution of Potassium chloride (Sigma-Aldrich)		KCl
3 % Hydrogen peroxide solution		H ₂ O ₂

Cell culture technique

After thawing the cells, we washed them twice in HS solution, using centrifugation for 5 min at 500g for precipitation. The culture vials with a capacity of 10 ml contained a standard complete medium of the composition MEM/DMEM + Glutamine + FCS + AB. A MEM was used for the MCF-7 cell culture in all experiments, and DMEM was used for the Vero culture. The reproduction providing the necessary number of cells took place in the thermostat at a temperature of 37 °C and in the presence of 5 % CO₂ in the gas phase. If necessary, we replaced the nutrient medium using as a criterion the level of cell viability in the trypan blue test and its morphology visualized using Olympus inverted microscope.

Determination of glucose oxidation pathway in cell cultures

The MCF-7 and Vero cells grew for 24 hours in a standard medium (1), in a medium with a glucose excess (2), and a medium without glutamine (3). The number of cells in each well was 2×10^5 .

We planted the pre-prepared MCF-7 and Vero cell cultures on 24-well plates at the rate of 100 μL/well using a standard complete medium of the composition MEM/DMEM + Glutamine + FCS + AB. Cultivation took place until ~ 95 % confluence in each well. Then the medium was replaced in each well to ensure the protocol of the experiment. Three variations of the MEM medium and three variations of the DMEM medium were necessary for this procedure.

The first variations made in eight wells on each plate were control ones, and they contained a standard complete medium. The subsequent eight wells contained glucose in addition to the standard complete medium. The third variant of medium did not contain glutamine in eight wells

on each tablet. After adding 2 mL of the appropriate medium to each well, the plates were cultured for 24 hours. Then the culture liquid was taken from the wells, centrifuged for 3 minutes at 500 g, and lactate was determined using a commercial Olvex Diagnosticum kit following the manufacturer's protocol. The optical density of the experimental and calibration samples was measured using an Olvex Diagnosticum spectrophotometer against a blank sample at a wavelength of 505 nm. The lactic acid concentration was expressed as

$$C = 3.3 E_e/E_c \text{ mM},$$

where E_e and E_c denote the optical densities of the experimental and calibration samples, respectively.

To provide the next stage of the study, we removed cells from the wells maintaining the marking adopted at the first stage and carried out the following experimental method.

Determination of oxygen uptake by cells

The measurement was performed using the cell metabolism analyzer Seahorse XFe24 (Agilent Technologies) by polarography.

Initially, the polarography medium, solutions of oligomycin, DNP, rotenone, KCl, and distilled water were incubated in a water thermostat at a temperature of 33 °C for 10 min. Next, 1 mL of a polarography medium containing 2×10^6 MCF-7/Vero cells were placed in a polarographic chamber. The respiration rate was sequentially recorded with this composition of the chamber, after the introduction of 100 μ L of oligomycin as an ATP synthase inhibitor, after the introduction of 100 μ L of rotenone to inhibit the I complex, and after the introduction of 100 μ L of DNF. Cellular respiration in each case was recorded for 3 min.

Statistical procedures

Statistical analysis was performed using the software package Statistica 12.0 (StatSoft Inc., USA). Distribution in the samples was expressed as mean \pm SEM. Statistical significance in differences between results was evaluated using Welch's *t*-test as two-tailed Student *t*-test with unequal variances. The differences were considered statistically significant when the *p*-value was less than 0.05.

3. Results

Lactate production under various cultivation conditions

The study showed that the lactate production by MCF-7 culture due to cultivation in a standard medium was significantly higher than by Vero cells (Table 2, Figure 1).

Table 2. Lactate concentration in MCF-7 and Vero cell cultures, mM/L

Cell line	Standard medium	Excess glucose	Without glutamine
MCF-7	9.55 \pm 0.13	8.58 \pm 0.28 #	9.63 \pm 0.25
Vero	7.21 \pm 0.11 *	7.03 \pm 0.10 *	7.18 \pm 0.07 *

Here and in Table 2, the * sign denotes significant differences in the values of the indicator between cell lines (*p* less than 0.05), the # sign denotes significant differences in the values of the indicator between the lines in an intact environment and its change.

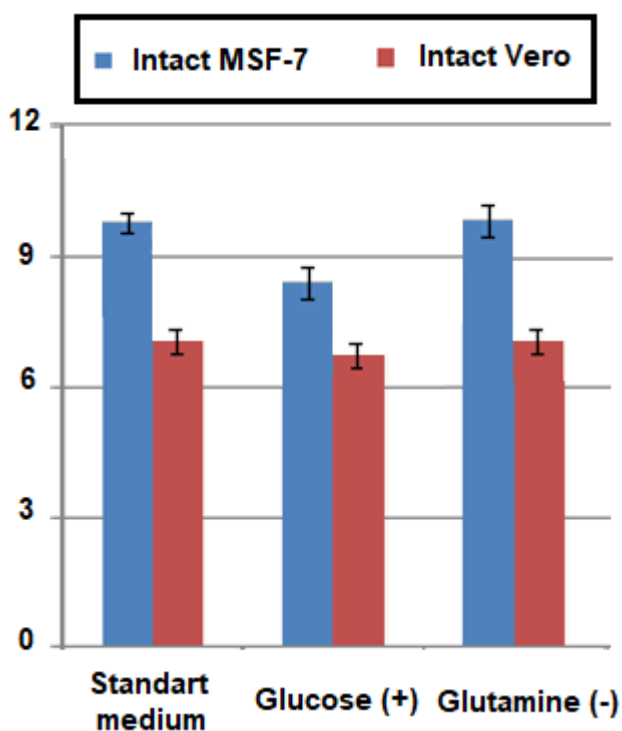


Fig. 1. Lactate production (mM/L of the final concentration) in the MCF-7 and Vero cell cultures under various cultivation conditions

Cultivation of MCF-7 in an environment with a glucose content of more than 1 g/L led to a decrease in lactate production by 9 %, while Vero cells practically did not change this production. The absence of glutamine in the culture medium did not significantly affect the lactate production for both MCF-7 and Vero cells.

Oxygen consumption under various cultivation conditions

Comparison of MCF-7 and Vero cultures showed a reduced O_2 consumption in MCF-7 culture, consistent with the ideas of a predominantly anaerobic energy flow in tumor cells (Table 3, Figure 2).

The measuring of cellular respiration after H_2O_2 treatment (negative control) gave the following results. The O_2 consumption decreased by 55.34% in comparison with the basic respiration data. The addition of oligomycin, DNF, or rotenone decreased O_2 consumption by 63.6 %, 53.0 %, and 42.67 %, respectively. After the damage by H_2O_2 , the differences between the cultures lost their statistical significance, proving the validity of the applied method.

Table 3. Respiration rates of MCF-7 and Vero cultures under various culture conditions (nM/s per 10^6 cells)

Cell line	Standard medium	Excess glucose	Without glutamine
Basic respiration			
MCF-7	11.90 ± 1.08	11.06 ± 1.04	11.30 ± 0.76
Vero	15.34 ± 0.90 *	13.89 ± 1.15 *	13.72 ± 0.97 *
Oligomycin			
MCF-7	7.98 ± 1.12	7.02 ± 1.07	7.50 ± 0.62
Vero	10.54 ± 1.05 *	9.11 ± 0.98	9.16 ± 1.36
DNP			
MCF-7	12.84 ± 0.97	12.70 ± 1.22	13.10 ± 1.02

Vero	16.55 ± 1.05 *	15.34 ± 1.23 *	14.67 ± 1.14
Rotenone			
MCF-7	8.90 ± 0.73	8.11 ± 1.24	8.01 ± 0.97
Vero	9.28 ± 0.83	8.33 ± 0.82	8.39 ± 1.41

The incubation of MCF-7 culture in the medium with increased glucose content was accompanied by a decrease in the respiration level of 1-5 %, which was insignificant. Similar comparisons in the Vero cell culture showed that in an environment with an increased glucose content, the indicators of basic respiration were 9.4 % lower than the control ones. The use of oligomycin, DNF, or rotenone led to the lowering of O₂ consumption by 13.6 %, 7.3 %, and 10.2 %.

Comparing intact MCF-7 cell culture with a culture incubated in the medium with the absence of glutamine revealed the decrease in oxygen concentration by an average of 1-4 % for all tests, which is insignificant. In the Vero cell culture, glutamine deprivation led to a 10.6 % decrease in basic respiration. O₂ consumption decreased by 13.1 %, 11.4 %, and 9.6 % in oligomycin, DNP, and rotenone tests, respectively.

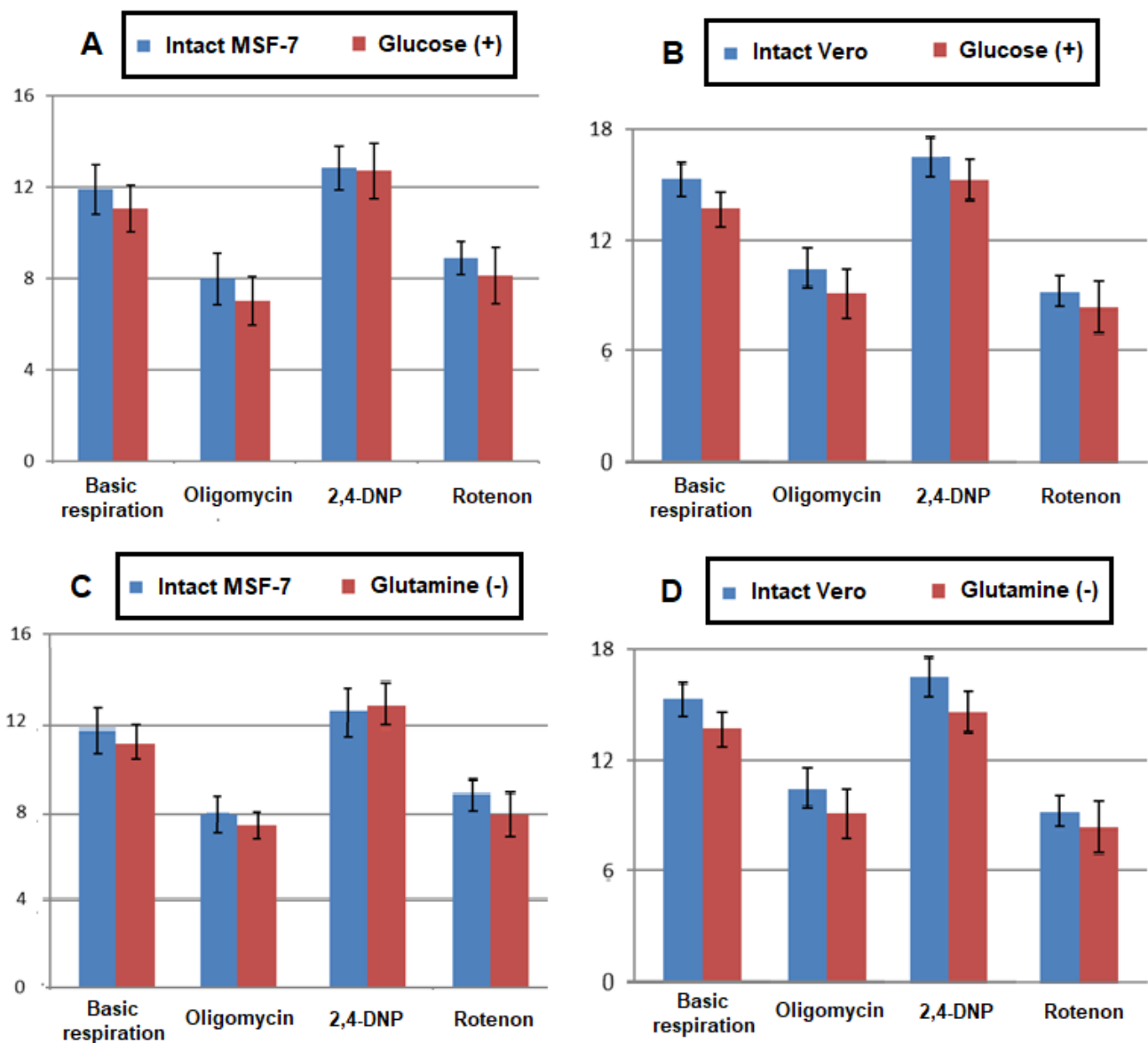


Fig. 2. Average O₂ consumption (nM/s per 10⁶ cells) in cell cultures under various culture conditions on polarography data. A. MCF-7 cell culture in medium with high glucose content. B. The same culture in medium without glutamine. C. Vero cell culture in medium with high glucose content. D. The same culture in medium without glutamine

4. Discussion

The number of oncological diseases has increased significantly. Therefore, it is necessary to identify new and study existing tumor cell lines to diagnose and treat this pathology effectively. All these events are closely related to the metabolic status of the cell, so a study of its metabolic pathways can provide the key to understanding the overall functionality of tumor cells (Jose et al., 2011).

Performing the work, we assumed that lactate production in tumor cells would be higher than in non-tumor cells due to the more intensity of metabolism, including the Warburg effect. Secondly, we considered it most likely that the glucose addition will increase the production of lactate, and the glutamine deprivation in the medium will lead to a decrease in the intensity of this process.

The first assumption was confirmed. In our experiments, the MCF-7 cells showed lactate production almost a third greater than Vero cells. The obtained data are consistent with the theory of metabolic reprogramming (the Warburg effect), characterized primarily by a shift in energy supply from mitochondrial oxidative phosphorylation to aerobic glycolysis. This is the most important distinguishing characteristics that cells acquire during tumor transformation. Lactate is a product of cell metabolism, which significantly increases when there is a lack of oxygen. Tumor cells, being in such conditions, actively produce lactate (Katzir et al., 2019).

As for the effects of glucose and glutamine, the production of lactate in the culture of MCF-7 cells did not increase in the first case, but it slightly decreased. In the second case, no changes were observed. In the culture of Vero cells, neither the glucose excess nor the glutamate absence led to a decrease in lactate production. The explanation of the obtained data may be that the glucose excess is already present in the nutrient medium that we took as the initial, of necessary to meet the energy needs of these cells.

Using polarography, we determined the crucial indicators of cellular respiration, which are vital for understanding the overall metabolic status of tumor cells (Traba et al., 2016).

We found that the basic respiration of tumor cells does not change in case of glucose added to the medium or glutamine absence in it, which may indicate that the MCF-7 culture uses internal mechanisms to switch metabolic pathways depending on environmental conditions. The indicator's value in the MCF-7 culture for all tests turned out to be lower than the same in the Vero culture by an average of 10-20 %. In contrast, Vero cells under these conditions significantly reduced the rate of O₂ consumption.

Oligomycin is an inhibitor of ATP synthase. When it is administered in cells, electrons are transferred along the respiratory chain with minimal ATP formation. Naturally, O₂ consumption, in this case, decreases (Salim et al., 2016). DNP partially uncouples oxidative phosphorylation, and therefore there is a compensatory increase in the O₂ consumption by cells. The rotenone application did not accompany differences in O₂ consumption in the cultures of tumor and normal cells. This fact resulted from its possible to completely inhibit complex I function, and the intensity of complex II functioning practically does not differ in tumor and non-tumor cells under these conditions.

The obtained data are consistent with the theoretical provisions explaining the peculiarities of cell metabolism, which show that glutamine can be used in providing cells with substrates to enhance the work of the respiratory chain and ATP synthesis. However, it should be noted that high activity of glycolytic pathway in tumor cells results in expression of glutamine effect in tumor cells less than in non-tumor ones (Zambrano et al., 2019).

Considering the data we obtained, new studies can be organized aimed at studying the mechanisms of rearrangement of the metabolism of tumor cell lines with changes in the concentrations of primary metabolites in the culture medium, for example, the study of inhibitors of the main metabolic pathways using 2-dehydroglucose, 3-bromopyruvate, aminotransferases, etc.

5. Conclusion

Our study found that lactate production in the MCF-7 tumor cell culture is significantly higher than in the Vero cell culture, which is in good agreement with the Warburg effect. The glucose excess is accompanied by a decrease in lactate production in the MCF-7 culture by almost 10 %, but not it is not typical for Vero cell culture. The glutamine absence in the culture medium does not significantly affect the change in lactate production for both Vero and MCF-7 cells.

In the culture of MCF-7 cells, glucose excess or glutamine absence during daily incubation did not statistically affect respiration, while in the culture of Vero cells, these changes were accompanied by a decrease in O₂ consumption by 10 % and 15 %, respectively.

The obtained data can be used to control the cultivation system and verify metabolic changes in testing new antitumor agents in vitro.

References

- [Alexandrova et al., 2019](#) – Alexandrova, R., Dinev, D., Gavriloval-Valcheva, I., Gavriloval, I. (2019). Cell cultures as model systems in breast cancer research. *Merit Res. J. Med. Med. Sci.* 7(2): 73-79.
- [Bhardwaj, He, 2020](#) – Bhardwaj, V, He, J. (2020). Reactive oxygen species, metabolic plasticity, and drug resistance in cancer. *Int. J. Mol. Sci.* 21(10): e3412. DOI: 10.3390/ijms21103412
- [Bray et al., 2018](#) – Bray, F., Ferlay, J., Soerjomataram, I. et al. (2018). Global cancer statistics 2018: GLOBOCAN estimates of incidence and mortality worldwide for 36 cancers in 185 countries. *CA Cancer J. Clin.* 68(6): 394-424. DOI: 10.3322/caac.21492
- [Butler et al., 2020](#) – Butler, L., Perone, Y., Dehairs, J. et al. (2020). Lipids and cancer: emerging roles in pathogenesis, diagnosis, and therapeutic intervention. *Adv. Drug Deliv. Rev.* 159: 245-293. DOI: 10.1016/j.addr.2020.07.013
- [Clegg et al., 2020](#) – Clegg, J., Koch, M.K., Thompson, E.W. et al. (2020). Three-dimensional models as a new frontier for studying the role of proteoglycans in the normal and malignant breast microenvironment. *Front. Cell Dev. Biol.* 8: e569454. DOI: 10.3389/fcell.2020.569454
- [Comsa et al., 2015](#) – Comsa, S., Cimpean, A.M., Raica, M. (2015). The story of MCF-7 breast cancer cell line: 40 years of experience in research. *Anticancer Res.* 35: 3147-3154.
- [Dai et al., 2017](#) – Dai, X., Cheng, H., Bai, Z., Li, J. (2017). Breast cancer cell line classification and its relevance with breast tumor subtyping. *J Cancer.* 8(16): 3131-3141. Doi: 10.7150/jca.18457.
- [DeSantis et al., 2016](#) – DeSantis, C.E., Siegel, R.L., Sauer A.G. et al. (2016). Cancer statistics for African Americans, 2016: Progress and opportunities in reducing racial disparities. *CA: Cancer J. Clin.* 66(4): 290-308. DOI: 10.3322/caac.21340
- [El-Sahli, Wang, 2020](#) – El-Sahli, S., Wang, L. (2020). Cancer stem cell-associated pathways in the metabolic reprogramming of breast cancer. *Int. J. Mol. Sci.* 21(23): e9125. DOI: 10.3390/ijms21239125
- [Gentric et al., 2017](#) – Gentric, G., Mieulet, V., Mechta-Grigoriou, F. (2017). Heterogeneity in cancer metabolism: new concepts in an old field. *Antioxid. Redox Signal.* 26(9): 462-485. DOI: 10.1089/ars.2016.6750
- [Jose et al., 2011](#) – Jose, C., Bellance, N., Rossignol, R. (2011). Choosing between glycolysis and oxidative phosphorylation: a tumor's dilemma? *Biochim. Biophys. Acta Bioenergetics.* 6(180): 552-561. DOI: 10.1016/j.bbabi.2010.10.012
- [Kang et al., 2018](#) – Kang, Y.P., Ward, N.P., DeNicola, G.M. (2018). Recent advances in cancer metabolism: a technological perspective. *Exp. Mol. Med.* 50(4): e31. DOI: 10.1038/s12276-018-0027-z
- [Katzir et al., 2019](#) – Katzir, R., Polat, I.H., Harel, M. et al. (2019). The landscape of tiered regulation of breast cancer cell metabolism. *Sci Rep.* 9(1): e17760. DOI: 10.1038/s41598-019-54221-y
- [Nelson, Cox 2014](#) – Nelson, D., Cox, M. (2014). Principles of biochemistry. *W.H. Freeman and Company.* 1115 p.
- [O'Shaughnessy et al., 2012](#) – O'Shaughnessy, J.A., Kaufmann, M., Siedentopf, F. et al. (2012). Capecitabine monotherapy: review of studies in first-line HER-2-negative metastatic breast cancer. *The Oncologist.* 17(4): 476-484. DOI: 10.1634/theoncologist.2011-0281
- [Osada et al., 2014](#) – Osada, N., Kohara, A., Yamaji, T. et al. (2014). The genome landscape of the African green monkey kidney-derived Vero cell line. *DNA Research.* 21(6): 673-683. DOI: 10.1093/dnares/dsu029
- [Park et al., 2020](#) – Park, J.H., Pyun, W.Y., Park, H.W. (2020). Cancer metabolism: phenotype, signaling and therapeutic targets. *Cells.* 9(10): e2308. DOI: 10.3390/cells9102308
- [Pattni et al., 2017](#) – Pattni, B.S., Jhaveri, A., Dutta, I. et al. (2017). Targeting energy metabolism of cancer cells: Combined administration of NCL-240 and 2-DG. *Int. J. Pharmaceutics.* 532(1): 149-156. DOI: 10.1016/j.ijpharm.2017.08.095

[Salim et al., 2016](#) – *Salim, A.A. Tan, L., Huang, X.-C. et al.* (2016). Oligomycins as inhibitors of K-Ras plasma membrane localization. *Org. Biomol. Chem.* 14(2): 711-715. DOI: 10.1039/c5ob02020d

[Traba et al., 2016](#) – *Traba, J., Miozzo, P., Akkaya, B. et al.* (2016). An optimized protocol to analyze glycolysis and mitochondrial respiration in lymphocytes. *J. Vis. Exp.* (117): e54918. DOI: 10.3791/54918

[Vander Heiden, DeBerardinis, 2017](#) – *Vander Heiden, M.G., DeBerardinis, R.J.* (2017). Understanding the intersections between metabolism and cancer biology. *Cell.* 168(4): 657-669. DOI: 10.1016/j.cell.2016.12.039

[Zambrano et al., 2019](#) – *Zambrano, A., Molt, M., Uribe, E., Mónica Salas, M. et al.* (2019). Glut 1 in cancer cells and the inhibitory action of resveratrol as a potential therapeutic strategy. *Int. J. Mol. Sci.* 13(20): e3374. DOI: 10.3390/ijms20133374

Copyright © 2021 by Academic Publishing House Researcher s.r.o.



Published in the Slovak Republic
 European Journal of Molecular Biotechnology
 Has been issued since 2013.
 E-ISSN: 2409-1332
 2021. 9(1): 12-25

DOI: 10.13187/ejmb.2021.1.12
www.ejournal8.com



Antimicrobial and Dyeing Studies of Some Novel Reactive Mono(bis mono), Tri(bis tri) Methine Cyanine Dyes based on Cyano Pyridazine Nucleus

Maha M. Gomaa^{a, *}, Safia A. Mahmoud^b

^a Aswan University, Aswan, Egypt

^b National Research Center, Giza, Egypt

Abstract

This study offers a synthesis of novel simple (bis simple) cyanine dyes and carbo (bis carbo) cyanine dyes having the nucleus of ethyl 5 cyano-4-methyl-1[3-amino-4-methyl(4-nitro) phenyl] 6-oxo-1,6-dihydropyridazine-3-ethyl carboxylate. The electronic absorption spectra of all the new synthesized simple (bis simple) and carbo (bis carbo) cyanine dyes investigated in 95 % (ethyl alcohol) to evaluate their sensitization properties. Studying spectral sensitization is very important in the case of cyanine dyes due to the extensive uses and applications of these dyes as photographic sensitizers in industry. The antibacterial and antifungal properties of some selected cyanine dyes were evaluated against two bacteria (*Escherichia coli*, *Staphylococcus aureus*), and two fungi (*Aspergillus flavus*, *Candida albicans*) and showed promising results. Structural characterization and confirmation carried out by mass spectra, elemental analysis, visible, ¹H NMR, and IR spectral data. Finally, dyeing process, and the fastness properties of the dyes were examined on polyester fabric. Polyester is the hydrophobic fibers and usually dyed with disperse dyes because of their high tinctorial strength and good fastness properties.

Keywords: cyanine dyes, synthesis, antimicrobial, spectral behavior, mono(bis mono), tri(bis tri) cyanine dyes, polyester fabric.

1. Introduction

Methine cyanine dyes are important species of organic heterocyclic dyes. This is due to the extraordinary applications and uses in a diverse and a board area, such as: biological applications (bactericidal, fungicidal, antimicrobial, anticancer and inhibitors for cell growth) (Cherkasov et al., 2010; Badran et al., 2007; Mohareb et al., 2007; Van-Der et al., 2006; Keisar et al., 2014; Vicini et al., 2002; Sener et al., 2018; Powar et al., 2009; Gomaa, 2014; Henary et al., 2013; Shindy et al., 2015; Shindy et al., 2016), as fluorescent labels, photosensitizers due to their antiradiation and antihalation (Ferreira et al., 2015; Li et al., 2012; Miki et al., 2017; Park et al., 2013; Xiang-Han et al., 2008; Hilal et al., 2007). In general, cyanine dyes are applied in modern high technology field due to their different physico-chemical and optical properties. Therefore, they have been used as optical recording and storage media (Sun et al., 2013; Sha et al., 2018), as potential sensitizers for photodynamic therapy(PDT) agent and in laser technologies (Upadhyayula et al., 2015; Abd El-Aal et al., 2004; Fayez, 2009). On the other hand, pyridazine derivatives are widely used as new luminescent (Alessio Raimondi et al., 2012), inhibitors of tau aggregation (Carlo Ballatore et al., 2012), mediated protein and peptide bioconjugation (Vijay Chudasama et al., 2011), antimicrobial (Asif et al., 2012), antihypertensive (Siddiqui et al., 2011; Rathish et al., 2012), anti-

* Corresponding author

E-mail addresses: mobarkmaha@yahoo.com (M.M. Gomaa)

inflammatory (Othman et al., 2014), antifungal (Ruso et al., 2014), and antimalarial (Asif et al., 2012; Onal et al., 2011). In this article, we developed and designed new pyridazine cyanine dyes (4a-d, 5a-d, 8a-d and 9a-d) to study their fluorogenic properties and antimicrobial evaluation to be used and/or applied in any of the wide areas of cyanine dyes, particularly as photographic sensitizers in photographic industry and/or as bactericidals. This paper also consider as an attempt to employ novel disperse dyes for dyeing fabric. The dyeing process showed promising results towards polyester fabric with good fastness properties.

2 Materials and methods

2.1. General experimental procedures

The melting points of the new synthesized dyes are measured by Electrothermal 15v, 45w I A 9100 melting point apparatus (Chemistry Department, University of Aswan, Egypt) and are uncorrected. Also the electronic absorption spectra carried out on visible spectrophotometer, spectro 24 RS Labomed, INC at (Aswan University). Elemental analysis data were recorded at the Microanalytical Center (Cairo University). ¹H NMR studies were measured on Varian Gemini-300 MHz NMR Spectrometer using DMSO as the internal reference solvent, and Infrared spectra were recorded with a FT/IR (4100 Jasco Japan) apparatus using KBr pellets at (Cairo University). Biological activity was carried out in Cairo University at Microbiology division, while the dyeing process studies on polyester were examined on Infra dyeing machine at National Research Centre (Dokki, Giza, Egypt).

2.2. Synthesis

The compounds were synthesized using the standard synthetic protocols. The procedures and their structure characterization data are given below.

2.2.1. Synthesis of ethyl 5 cyano-4-methyl-1[3-amino-4-methyl(4-nitro)phenyl]-6-oxo 1,6-dihydropyridazine-3-ethyl carboxylate (3a, b).

This compound was synthesized by using the reference described earlier (Scheme 1) (Abdalla, 2015).

2.2.2. Synthesis of ethyl 5 cyano-4-methyl-1[3-amino-4-methyl(4-nitro)phenyl]-1,6-dihydropyridazine-3-ethyl carboxylate 6(2) monomethine cyanine dyes (4a-d).

An ethanolic solution of equimolar ratio of compound (3a, b) (0.01 mmol) and N-iodoethane quaternary salts of α -picoline and/or quinaldine (0.01 mmol) was heated with (3-7 drops) of piperidine for 7-10 hrs. The hot product was filtered off, concentrated, neutralized and precipitated using crushed ice. The crude product was crystallized from ethanol and the collected crystals were dried (4a-d), and tabulated in Table 1.

2.2.3. Synthesis of ethyl 5-cyano-4-methyl-1[3-amino-4-methyl(4-nitro)phenyl]-1,6-dihydropyridazine-3-ethyl carboxylate 3,6(2)bis monomethine cyanine dyes (5a-d).

There are two different routes employed to synthesize these series of cyanine dyes.

Route (1): A few mls of piperidine were added to an ethanolic solution (30 ml) of (3a, b) (0.01 mmol) and N-iodoethane quaternary salts of α -picoline and/or quinaldine (0.02 mmol). This mixture was refluxed for 6-10 hrs, filtered hot, concentrated, cooled, and neutralized with acid. The newly dyes (5a-d) were collected and crystallized by using a suitable solvent. The data is given in Table 1.

Route (2): A mixture of the previously synthesized monomethine cyanine dyes (4a-d) (0.01 mmol) and equimolar ratios of N-iodoethane quaternary salts of α -picoline and/or quinaldine (0.01 mmol) was dissolved in ethanol (35 ml). To this mixture, (2-6 drops) piperidine were added and refluxed for 3-6 hrs. The product was filtered hot, concentrated, cooled, neutralized and precipitated by using crushed ice. The crude product was recrystallized from ethanol to get the same compounds obtained from route (1), characterized by melting points, mixed melting points, same IR and ¹H NMR spectral.

2.2.4. Synthesis of intermediate (6a, b)

A dissolution of a mixture of equimolar ratios (0.01 mmol) of (3a, b) and acetaldehyde (0.01 mmol) was conducted in ethanol (20 ml) and 1-2 mls of piperidine were added. The reaction mixture was refluxed for 6 hrs, filtered hot, concentrated, cooled and precipitated by adding cold water. The precipitates (6a, b) were collected, dried and crystallized from ethanol. The results are recorded in Table 1.

2.2.5. Synthesis of intermediate (7a, b)

Two different routes are employed to prepare (7a, b).

Route 1: Adding piperidine (1-2 mls) to an ethanolic solution (30 ml) of (3a, b) (0.01 mmol) and bimolar ratio of acetaldehyde (0.02 mmol). The mixture was heated under reflux for 6 hrs, filtered off while hot, concentrated, cooled and poured in ice water. The crude product was filtered off, washed with water and crystallized from ethanol. The results are listed in [Table 1](#).

Route 2: Dissolving equimolar ratios (0.01 mmol) of (6a, b) and acetaldehyde (0.01 mmol) in ethanol (20 ml) and adding (6-9 drops) of piperidine to the mixture. The reaction mixture was refluxed for 6 hrs, filtered hot, concentrated, cooled and precipitated by adding cold water. The obtained precipitate was dried and crystallized from ethanol to give the same compound (7a, b) obtained by route(1), characterized by melting points, mixed melting points, as well as same IR and ¹H NMR spectral data.

2.2.6. Synthesis of ethyl 5-cyano-4-methyl-1[3-amino-4-methyl (4-nitro)phenyl]-1,6-dihydropyridazine-3-ethyl carboxylate 6(2)trimethine cyanine dyes (8a-d)

An equimolar ratios of compound (6a, b) (0.01 mmol) and N-iodoethane quaternary salts of α -picoline and/or quinaldine (0.01 mmol) in ethanol (35 ml) containing piperidine (1 ml) heated under reflux for 7-9 hrs, filtered hot, concentrated and precipitated by adding ice. The obtained precipitate was filtered off, washed with water, and then crystallized from ethanol to give (8a-d).

The results are listed in [Table 1](#).

2.2.7. Synthesis of ethyl 5-cyano-4-methyl-1[3-amino-4-methyl(4-nitro)phenyl]-1,6-dihydropyridazine-3-ethyl carboxylate 3,6(2)bis trimethine cyanine dyes (9a-d)

A few mls of piperidine were added to an ethanolic solution (30 ml) of (7a, b) (0.01 mmol) and N-iodoethane quaternary salts of α -picoline and/or quinaldine (0.02 mmol). This mixture was refluxed for 6-9 hrs, filtered hot, concentrated, cooled, and neutralized with acid. The newly dyes (9a-d) were collected and crystallized by using a suitable solvent. The data are given in [Table 1](#).

2.3. Absorption spectroscopy

The absorption spectra of the new dyes were examined in their ethanolic solution (95 % ethyl alc.) and recorded by using [10^{-4} M concentration of the dye, 1 cm quartz cell].

2.4. Biological activity

Antimicrobial (antibacterial, antifungi) activity of the tested sample (4a, 4b, 4c, 4d, 5a, 5b, 5d, 8a, 8b, 8d, 9a, 9b, 9c, 9d) was studied and determined by using the modified method of Kirby-Bauer disc diffusion ([Ballatore et al., 2012](#); [King et al., 2010](#)). The tested dyes were dissolved in DMSO to obtain a final concentration (1 mgm/ml). We use 100 μ l of the test fungi/bacteria to grow in 10 ml of fresh media till they reach about 10⁵ cells/ml for fungi or 10⁸ cells/ml for bacteria. Then, 100 μ l of microbial suspension was distributed into Mueller-Hinton agar plates. We should put into consideration the depth of agar in the disc diffusion method ([El-Mashad et al., 2012](#); [Mohamed et al., 2014](#)). Finally, biological activity for each sample was examined on surface – seeded nutrient agar medium with the prepared susceptible disc. Biological effect and the bacterial strains are reported in [Table 3](#).

2.5. Fabric

El-Mahalla El-Kobra Company, Egypt kindly supplied Polyester fabric, mill-scoured and bleached. The fabrics were scoured at 50 °C for 30 min, L:R (1:50), 2 g/L of nonionic detergent solution (Hostapal; Clariant, Swiss), and 2 g/L of Na₂CO₃. **Then, they are rinsed with cold water and dried at room temperature.**

Dyeing Method

Dyeing experiments were carried out in two separate steps. In the first step, polyester fabric was dyed with prepared disperse dyes. Dyeing process takes place at pH= 5 (using acetic acid), while liquor ratio equal 1:50. Dye bath consisted of 1 % of dye, and Matexil DA-N (supplied by ICI Company, UK) as dispersing (1 ml/L). Dyeing process started at 40 °C, the temperature was raised to 130 °C for 60 min. After dyeing, the samples were washed with cold water and a reduction cleaning was made with sodium hydroxide (2 g/L), hydrosulphite (2 g/L) at 60 °C for 10 min. Then, the samples were treated by acetic acid (1 ml/L) at 40 °C for 5 min, followed by cold water and dried at room temperature ([Tarek Aysha et al., 2015](#); [Tarulata et al., 2011](#)).

2.6. Color Measurements of the dyed samples

Color Strength

The colorimetric analysis of the dyed samples was performed using a Hunter Lab ultra Scan® PRO spectrophotometer. The corresponding colour strength value (K/S) was assessed by applying the Kubelka Munk equation as follows (Kubelka et al., 1931):

$$K/S = \frac{(1-R)^2}{2R} \quad (1)$$

Where,

R = decimal fraction of the reflection of the dyed fabric,

K = absorption coefficient, and S = scattering coefficient

Fastness testing

The dyed samples were subjected to rubbing, washing, sublimation, perspiration and light according to ISO methods [ISO 105-EO₄ (1989), ISO 105-X12 (1987), ISO 105-CO₄ (1989) and ISO 105-BO₂(1988)].

3. Results and discussion

3.1. Synthesis

Reaction of ethyl-5cyano-4-methyl-1[3-amino-4-methyl(4-nitro)phenyl]6-oxo-1,6-dihydropyridazine 3-ethyl carboxylate (3a, b) with N-iodoethane quaternary salts of (α-picoline and/or quinaldine) in equimolar ratios in ethanol containing few drops of piperidine afforded to the monomethine cyanine dyes (4a-d), Scheme 1. These compounds (4a-d) were employed as new heterocyclic starting material compounds to synthesize bis monomethine (5a-d) through its reaction with 1-ethyl 2-methyl pyridinium-2-yl salt and/or 1-ethyl 2-methyl quinolinium-2-yl salt in (1:1 molar ratios) and ethanol containing (3-5 drops) of piperidine, achieving 3,6(2)bis monomethine cyanine dyes (5a-d), route(2), Scheme 1 (Appendix 1). Bis monomethine cyanine dyes (5a-d) were chemically confirmed through condensation of (3a, b) with N-iodoethane quaternary salts of α-picoline, and/or quinaldine in (1:2 ratio) using the same previous conditions to obtain the same compound (5a-d) route (1), Scheme (1). On the other hand, condensation reaction between (3a, b) with equimolar and/or biomolar (route 1) ratio of acetaldehyde in the presence of ethanol and piperidine achieved the corresponding compounds (6a, b, 7a, b), Scheme 1. The intermediate (7a, b) was chemically confirmed through condensation of (6a, b) with acetaldehyde in (1:1) ratio (route 2) under ethanol/piperidine catalysis to obtain the same compound (7a, b). Compounds (6a, b, 7a, b) were employed to synthesize some novel tri (bis tri) methine cyanine dyes (8a-d, 9a-d) through condensation of the new synthesized compound (6a, b, 7a, b) with equimolar and/or bimolar ratio (route 1) of N-iodoethane quaternary salts of [α-picoline and/or quinaldine] under piperidine/ethanol condition, producing the corresponding, 6(2) tri and 3,6(2)bis trimethine cyanine dyes (8a-d, 9a-d), Scheme 1).

3.2. Spectral characterization

Dyes (4a-d), (5a-d), (8a-d) and (9a-d) are highly colored compounds(ranging from brown to violet) and soluble in polar solvents concomitantly with intense or slight greenish-red fluorescence. Structure-spectra studies of all the new mono (bis mono) and tri (bis tri) methine cyanine dyes (4a-d, 5a-d, 8a-d, 9a-d) were carried out by measuring their visible electronic absorption spectra in ethanolic solutions Table 1 (Scheme 1, 2).

The electronic absorption spectra of monomethine (4a-d), and bis monomethine (5a-d) cyanine dyes exhibit absorption bands in the visible regions (370-560 nm) and (370-568 nm), respectively. On the other side, trimethine (bis trimethine) cyanine dyes recorded absorption bands in regions (370-620 nm) and (370-630 nm) (Table 1). This indicates that the value of absorption bands, position and molar extinction coefficient was influenced by several factors, such as: the nature of heterocyclic quaternary residue (A), electron withdrawing or donating groups present in the molecule, the number of methine units and the number of charge transfer pathway (Powar et al., 2009; Gomaa, 2014; Henary et al., 2013; Shindy et al., 2015; Gomaa et al., 2012; Ahmed et al., 2018; Shindy et al., 2019; Shindy et al., 2015; Shindy, 2018; Shindy et al., 2017; Shindy et al., 2015; Soriano et al., 2016; Shindy et al., 2018; Gomaa, 2019). So, the absorption spectra of dyes (4b, d), (5b, d), (8b, d) and (9b, d) is a red-shifted to dyes (4a, c), (5a, c), (8a, c) and (9a, c) respectively. This back to the extensive π-delocalization and conjugation

in the quinoline ring in dyes (4b, d), (5b, d), (8b, d) and (9b, d) than those of pyridine ring in (4a, c), (5a, c), (8a, c) and (9a, c). Additionally dyes (4c, d), (5c, d), (8c, d) and (9c, d) are a bathochromically shifted to their analogous (4a, b), (5a, b), (8a, b) and (9a, b) respectively. This is due to the positive inductive effect of (CH₃) group in dyes (4c, d), (5c, d), (8c, d) and (9c, d).

Consequently, dyes have two charge transfer pathways (5a-d, 9a-d) are highly bathochromically shifted if compared with dyes containing one charge transfer pathway (4a-d, 8a-d). This is due to the increasing π -delocalization and extra conjugation (Table 1, Scheme 2, Appendix 2).

Finally (trimethine and bis trimethine) cyanine dyes are red shifted compared to (mono and bis mono) cyanine dyes. This back to the increasing of both number of methine groups and conjugation between the two heterocycles (nitrogen) (Table 1, Scheme 2).

Table 1. Characterization of compounds (4a-9d)

Comp. No.	Nature of products			Molecular formula (M. Wt.)	Analysis %						Absorption spectra in 95% ethanol solution	
	Colour	Yield %	M.P. °C		Calculated			Found			λ_{max} (nm)	ϵ_{max} (mol ⁻¹ cm ²)
					C	H	N	C	H	N		
4a	Brownish red	90	190-194	C ₂₃ H ₂₂ N ₅ O ₄ I 559	49.37	3.93	12.52	49.11	3.99	12.3	447	18800
4b	Deep brown	77	224	C ₂₇ H ₂₄ N ₅ O ₄ I 609	53.2	3.94	11.49	53	3.74	11.53	515,550	16760,17980
4c	Brownish red	75	>300	C ₂₄ H ₂₂ N ₅ O ₂ I 543	53.03	4.78	12.89	53.17	4.88	12.93	370,395,417,450	12910,8330,9110,9630
4d	Deep brown	70	>300	C ₂₈ H ₂₈ N ₅ O ₂ I 593	56.66	4.72	11.8	56.49	4.8	11.88	430,460,560	20000,19450,12500
5a	Brownish red	85	225	C ₃₁ H ₃₂ N ₆ O ₃ I ₂ 790	47.08	4.05	10.63	47.11	4.15	10.66	455	23110
5b	Dark brown	79	220-225	C ₃₃ H ₃₆ N ₆ O ₃ I ₂ 890	52.58	4.04	9.43	52.7	4.19	9.33	450 sh,517,555	20060,18040,19540
5c	Brownish red	87	>300	C ₃₂ H ₃₆ N ₆ OI ₂ 774	49.61	4.65	10.85	49.50	4.70	10.90	370,470	1660,6500
5d	Greenish	78	295-300	C ₄₀ H ₄₂ N ₆ OI ₂ 874	54.91	4.57	9.61	54.83	4.66	9.55	370,460,568	9400,1100,5900
6a	Deep red	70	120-125	C ₁₇ H ₁₄ N ₄ O ₅ 354	57.62	3.95	15.81	57.53	3.82	15.70	-----	-----
6b	Purple	77	240-245	C ₁₈ H ₁₈ N ₄ O ₃ 338	63.90	5.32	16.56	63.88	5.43	16.66	-----	-----
7a	Pale brown	83	110-115	C ₁₉ H ₁₆ N ₄ O ₅ 380	60	4.21	14.73	60.20	4.33	14.71	-----	-----
7b	Pale Violet	77	180-183	C ₂₀ H ₂₀ N ₄ O ₃ 364	65.93	5.49	15.38	65.90	5.33	15.19	-----	-----
8a	Deep red	87	230-235	C ₂₅ H ₂₄ N ₅ O ₄ I 585	51.28	4.10	11.96	51.34	4.27	11.88	440,480	18200,5800
8b	Deep violet	73	200	C ₂₉ H ₂₆ N ₅ O ₄ I 635	54.80	4.09	11.02	54.69	4.19	11.18	370,514,560	18600,13300,16300
8c	Deep brown	85	300	C ₂₆ H ₂₈ N ₅ O ₂ I 569	54.83	4.92	12.30	54.80	4.86	12.44	370,440,465,480	16300,14400,9900,9320
8d	Deep violet	80	275-280	C ₃₀ H ₃₀ N ₅ O ₂ I 619	58.15	4.84	11.30	58.20	4.79	11.47	370,440,565,620	16200,13100,6700,4300
9a	Reddish violet	80	200	C ₃₃ H ₃₆ N ₆ O ₃ I ₂ 842	49.88	4.27	9.97	49.72	4.37	9.86	370,490	18010,17870
9b	Deep violet	78	180-185	C ₄₃ H ₄₆ N ₆ O ₃ I ₂ 942	54.77	4.24	8.91	54.67	4.15	8.83	460,517 sh,565	19400,16760,17940
9c	Deep red	74	100-105	C ₃₆ H ₄₀ N ₆ OI ₂ 826	52.30	4.84	10.16	52.20	4.76	10.10	370,415 sh,440,500	17320,11300,10900,6350
9d	Deep violet	78	295-300	C ₄₄ H ₄₄ N ₆ OI ₂ 926	57.01	4.75	9.07	57.12	4.81	8.99	540,580,630	18750,17400,11300

Table 2. Characterization of compounds (4a-9c)

Comp. No.	IR (KBr, cm ⁻¹)	¹ H NMR (DMSO, δ); & (Mass data)
4a	1452(C=N).1595(C=C) 2920-2851(quaternary salt).	0.84 (m, 3H, CH ₃ , N-pyridinium), 1.50 (m, 3H, CH ₃ of ethoxy), 2.8 (s, 3H, CH ₃). 3.31 (s, 2H, CH ₂ , N-pyridinium). 4.56 (q, 2H, CH ₂ of ethoxy). 6.58-8.98 (m, 9H, 8 Ar-H + =CH-).
5a	1445(C=N).1600(C=C). 2920-2852(quaternary salt).	0.85 (m, 6H, 2CH ₃ , N-pyridinium), 1.44 (m, 3H, CH ₃ of ethoxy). 2.72 (s, 3H, CH ₃). 3.31-4.31 (m, 4H, 2CH ₂ , N-pyridinium), (m, 2H, CH ₂ of ethoxy). 7.40-8.25 (m, 14H, 12 Ar-H + 2=CH-).

7a	1481(C=N).1295(C-N). 1627 (C=C).1737(C=O)aldehy -dic.2925 (C-H) aldehydic	1-1.48 (m,3H,CH ₃ of ethoxy), 2.51 (s,3H,C H ₃), 3.3- 4.5 (q,2H,CH ₂ of ethoxy), 6.85 (m, 6H,4Ar-H+2=CH-), 10.52 (s,2H,2CHO group). M ⁺ : 380
8a	1481(C=N).1627(C=C) 2909,2807(quaternary salt).	1.23 (m, 3H, CH ₃ , N-pyridinium). 1.53 (t, 3H, CH ₃ of ethoxy). 2.60 (s,3H,CH ₃) 3.31 (s, 2H, CH ₂ , N-pyridinium). 4.55 (q, 2H, CH ₂ of ethoxy). 6.57-8.93 (m, 11H, 8Ar-H +3=CH-). (8d): M ⁺ :621
9c	1450(C=N).1588-1661(C=C) 2816(quaternary salt).3213((NH ₂))	1.0-1.54 (m, 6H, 2CH ₃ , N-pyridinium), (m, 3H, CH ₃ of ethoxy), 2.4-2.8(s, 6H, 2CH ₃), 3.5(s, 2H, NH ₂), 4.55-4.62 (m, 4H, 2CH ₂ ,N-pyridinium), (m,2H,CH ₂ of ethoxy 7.95-9.03(m, 17H, 11Ar-H + 6=CH-).

3.3. Biological activity

The antimicrobial (antibacterial, antifungi) activity for some selected newly synthesized cyanine dyes (4a-d; 5a, b, d; 8a, b, d; 9a-d) was studied against some bacterial strains (*Escherichia coli*, *Staphylococcus aureus*) and some fungi strains (*Aspergillus flavus*, *Candida albicans*), [Table 3](#).

So, in this study, the antimicrobial activity of all tested dyes showed higher inhibition zone diameter in the case of *staphylococcus aureus* (G⁺) compared with *Escherichia coli* (G⁻). This reflects their ability to be used as antibacterial active against this bacterial strain ([Table 3](#)). Comparison between the antibacterial activity of the bis trimethine cyanine dye (9d) and the bis monomethine cyanine dyes (5d) showed that, the latter dye (5d) possess higher potency as antibacterial activity than the former (9d) ([Table 3](#)). This could be related to the increasing number of methine groups in dye (9d). The presence of nitro groups largely increased the activity of dyes (4b, 8b and 9b) against the bacterial strains. This may be attributed to the electron accepting character of nitro group. Replacing the NO₂ group in cyanine dye (5b) by CH₃ group to obtain dye (5d) increasing for the inhibition zone diameter for (*Escherichia coli*, *Staphylococcus aureus*) bacterial strains ([Table 3](#)). This is due to the electron pushing character of CH₃ group in dye (5d). The antibacterial activity of the dye (5d) possesses higher inhibition zone diameter against bacterial strains compared with the other dyes ([Table 3](#)). This gives it the opportunity to use as antimicrobial active. Furthermore, most of the dyes are biologically inactive against tested fungi strains (*Aspergillus flavus*, *Candida albicans*), except 4b, 4d, 5d, 8b, 9b and 9d. Dye (4d) gave the highest inhibition zone diameter against (*Aspergillus flavus*) and this enables it to be used as antifungi. Comparing the antimicrobial activity of [mono-methine(4b), trimethine(8b)]cyanine dyes with their analogous [bis mono (5b), bis tri(9b)]methine cyanine dyes indicate that (mono, tri) have higher value of inhibition zone diameter than (bis mono, bis tri). This may be related to both hydrophilic and hydrophobic structural equilibria of the tested dyes ([Table 3](#)).

Finally, the antimicrobial activity of the synthesized cyanine dyes (4a-d, 5a, b, d; 8a, b, d; 9a-d) increase/or decrease to give higher/or lower inhibition zone diameter depending upon: electron accepting (NO₂) or electron donating (CH₃), type of quaternary salt residue (A), kind of (bacterial strains and fungi), number of methine groups and the number of charge transfer pathway [Table 3](#).

Table 3. Biological activity of some newly synthesized compounds

Sample		Inhibition zone diameter (mm/mg sample)			
		Escherichia coli (G ⁻)	Staphylococcus aureus (G ⁺)	Aspergillusflavus (fungus)	Candida albicans (fungus)
Control: DMSO		0.0	0.0	0.0	0.0
Standard	Ampicillin Antibacterial agent	22	18	---	---
	Amphotericin B Antifungal agent	---	---	17	19
	4a	0	0	0	0
	4b	16	17	0	9
	4c	0	0	0	0
	4d	0	0	33	0
	5a	0	0	0	0
	5b	14	15	0	0
	5d	24	26	0	10
	8a	0	0	0	0
	8b	21	22	9	13
	8d	10	0	0	0
	9a	9	10	0	0
	9b	18	20	0	9
	9c	9	10	0	0
	9d	17	22	0	10

3.4. Color strength

Color strength K/S, L, a, b, and ΔE values of polyester fabrics dyed by disperse dyes are set out in Table 4. Dyeing was carried out at 130°C, L. R 1:50,1 % (w.o.f), and at pH 4.5 for 60 min. CIE (L*, a*, b*) system was used to measure the color coordinates, where (L*) indicates lightness or darkness values which range from 0 to 100, (a*) range from green to red, and (b*) range from yellow (positive) to blue (negative). Table 4 showed that dyed polyester fabric recorded high L* value (59.93-81.68), negative and low a* (-1.53-8.42), and b* value (47.72-48.65) for dyed polyester fabric. In addition, this table stated that the color strength K/S values of dyed polyester refer to the absorbance of dye on the surface of the fiber. Moreover, this indicated that the polyester fabrics have high affinity for some synthesized disperse dyes and not for all dyes.

Table 4. Color strength K/S, L, a, b, and ΔE value of polyester fabrics dyed by disperse dyes

Samples	K/S	L	A	B	ΔE
4a	8.12	74.36	-23.5	36.45	45.62
4b	13.49	65.95	-1.83	35.58	47.45
4c	2.48	62.67	5.15	8.97	28.08
4d	2.62	64.08	5.93	11.68	28.8
5a	13.27	71.01	-1.16	42.17	51.87
5b	14.54	68.68	-1.53	39.89	50.43
6a	16.88	59.93	8.42	47.72	61.11
7a	13.49	70.06	-2.21	48.65	57.17
8a	4.54	81.68	-3.67	21.04	29.48
8b	5.34	67.62	-0.43	14.63	28.46

8d	2.26	67.11	5.57	9.83	25.3
9a	2.61	70.83	6.6	15.42	27.69
9b	7.14	69.28	-2.88	27.05	38.47
9c	8.34	70.69	-5.04	37.11	46.1
9d	2.16	71.54	5.3	6	19.48

3.5. Fastness properties

The polyester fabric dyed with disperse dyes was tested to washing, perspiration, rubbing, sublimation, and light. The results are shown in Table 5. From Table 5, it can be seen that the washing fastness of polyester fabric dyed with all disperse dyes ranges from good to very good (4-5). Moreover, both alkaline and acidic perspiration test gave the same results ranged from good to very good (4-5). Dry and wet crocking test was similar to both washing and perspiration fastness which gave very good results (4-5). On the other hand, the light fastness properties were very good (3-5). In addition, Table 5 showed that thermal fixation at 180°C gave better results than thermal fixation at 210°C.

Table 5. Fastness properties of polyester fabrics dyed by disperse dyes

Dyes	Washing fastness			Rubbing fastness		Perspiration fastness						Sublimation		Light fastness
	Alt.	St.*	St.**	Dry	Wet	Acidic			Alkaline			210°C	180°C	
						Alt.	St.*	St.**	Alt.	St.*	St.**			
4a	4-5	4-5	4-5	4-5	4-5	4-5	4-5	4-5	4-5	4-5	4-5	3	3-4	4
4b	4-5	4-5	4-5	4-5	4-5	4-5	4-5	4-5	4-5	4-5	4-5	3	3-4	3-4
4c	4-5	4-5	4-5	4-5	4-5	4-5	4-5	4-5	4-5	4-5	4-5	4	4-5	4-5
4d	4-5	4-5	4-5	4-5	4-5	4-5	4-5	4-5	4-5	4-5	4-5	4	4-5	4-5
5a	4-5	4-5	4-5	4-5	4-5	4-5	4-5	4-5	4-5	4-5	4-5	3	3-4	3-4
5b	4-5	4-5	4-5	4-5	4-5	4-5	4-5	4-5	4-5	4-5	4-5	3	3-4	4
6a	4-5	4-5	4-5	4-5	4-5	4-5	4-5	4-5	4-5	4-5	4-5	3	3-4	3-4
7a	4-5	4-5	4-5	4-5	4-5	4-5	4-5	4-5	4-5	4-5	4-5	3	3-4	3-4
8a	4-5	4-5	4-5	4-5	4-5	4-5	4-5	4-5	4-5	4-5	4-5	3	3-4	3-4
8b	4-5	4-5	4-5	4-5	4-5	4-5	4-5	4-5	4-5	4-5	4-5	3	3-4	3-4
8d	4-5	4-5	4-5	4-5	4-5	4-5	4-5	4-5	4-5	4-5	4-5	4	4-5	4-5
9a	4-5	4-5	4-5	4-5	4-5	4-5	4-5	4-5	4-5	4-5	4-5	3	3-4	3-4
9b	4-5	4-5	4-5	4-5	4-5	4-5	4-5	4-5	4-5	4-5	4-5	3	3-4	4
9c	4-5	4-5	4-5	4-5	4-5	4-5	4-5	4-5	4-5	4-5	4-5	4	4-5	4
9d	4-5	4-5	4-5	4-5	4-5	4-5	4-5	4-5	4-5	4-5	4-5	4-5	4-5	4-5

St.* Staining on cotton

St.** Staining on wool

Alt. Alteration in color

4. Conclusion

In this article, sixteen new [mono(bis mono) and tri(bis tri)] methine cyanine dyes were synthesized. The fastness properties, dyeing process, antimicrobial activity and absorption of most dyes were examined and recorded.

1. The UV absorption spectra of monomethine cyanine (4a-d), bismonomethine (5a-d), trimethine (8a-d) and bis trimethine (9a-d) cyanine dyes underwent displacements towards (batho and/or hypso) chromic shifted bands due to:

- a) The nature of the quaternary salt in the molecule;
- b) Number of methine groups;
- c) Charge transfer pathways;
- d) Electron donating group (CH₃) and withdrawing (NO₂);
- e) Intensity of colours of (bis tri, tri, bis mono, and mono)methine cyanine dyes depending upon the presence of two mesomeric structures (A) and (B), **Scheme 2**.

2. Dyes can be used in photographic industry as photographic sensitizers due to spectral properties, and as antimicrobial agents against some bacterial and fungi strains.

3. Finally, fastness properties and dyeing process of (bis tri, tri, bis mono and mono) methine cyanine dyes were tested on polyester fabrics.

5. Acknowledgments

Sincere appreciation to all members of the Chemistry Department in Aswan University and the National Research Centre (Giza, Egypt) for their encouragement and support during this work.

References

- Cherkäsov et al., 2010 – Cherkäsov, D., Biet, T., Baumil, E., Ttraut W., Lohoff, M. (2010). New nucleotide analogues with enhanced signal properties. *Bioconjugate Chem.* 21: 122-129. DOI: 10.1021/bc900364f
- Badran et al., 2007 – Badran, M.M., Moneer, A.A., Refaat, H.M., El-Malah, A.A. (2007). Synthesis and antimicrobial activity of novel quinoxaline derivatives. *J. Chin. Chem. Soc.* 54(2): 469-478. DOI: <https://doi.org/10.1002/jccs.200700066>
- Mohareb et al., 2007 – Mohareb, R.M., Ho, J.Z., Alfarouk, F.O. (2007). Synthesis of thiophenes, azoles and azines with potential biological activity by employing the versatile heterocyclic precursor N-benzoylcyano acetylhydrazine. *J. Chin. Chem. Soc.* 54: 1053-1066. DOI: <https://doi.org/10.1002/jccs.200700152>
- Van-Der et al., 2006 – Van-Der, S., Blunt, J., Munro, M. (2006). Spiro-Mamakone A: A unique relative of the spiro-bisnaphthalene class of compounds. *Org. Lett.* 8: 2059-2061. DOI: <https://doi.org/10.1021/01060434k>
- Keisar et al., 2014 – Keisar, O.R., Finfer, E.K., Ferber, S., Finaro, R., Shabat, D. (2014). Synthesis and use of Qcy7-derived modular probes for the detection and imaging of biologically relevant analytes. *Nature Protocols.* 9(1): 27-36. DOI: 10.1038/nprot.2013.166
- Vicini et al., 2002 – Vicini, P., Zani, F., Cozzini, P., Doytchinova, I. (2002). Hydrazones of 1,2-benzisothiazole hydrazines: synthesis, antimicrobial activity and QSAR investigation. *Eur. J. Med. Chem.* 37: 553. DOI: [https://doi.org/10.1016/S0223-5234\(02\)01378-8](https://doi.org/10.1016/S0223-5234(02)01378-8)
- Sener et al., 2018 – Sener, N., Mohammed, H.J.A., Yerlikaya, S., Celik Altunoglu, Y., Gur, M., Baloglu, M.C, Sener, I. (2018). Anticancer, antimicrobial, and DNA protection analysis of novel 2,4-dihydroxyquinoline dyes. *Dyes and Pigments.* 157: 11-19. DOI: <https://doi.org/10.1016/j.dyepig.2018.04.040>
- Powar et al., 2009 – Powar, M.J., Burungle, A.B., Karale, B.K. (2009). Synthesis and antimicrobial activity of spiro[chromeno[3,3-d][1,2,3]thiadiazole-4,1-cyclohexane, spiro[chromeno]-[4,3-d][1,2,3]selenadiazole-4,1-cyclohexane and spiro [chromon-2,1-cyclohexane]4-one-5-spiro-4-acetyl-2(acetylamino)-Δ²-1,3,4-thiadiazolines compounds. *Arkivoc.* 9: 97-107. DOI: <https://doi.org/10.3998/ark.5550190.0010.do8>
- Gomaa, 2014 – Gomaa, M.M. (2014). Oxonium heterocyclic quinone in the synthesis of some cyanine dyes and their antimicrobial activity. *Eur. J. Chem.* 5(3): 463-468. DOI: <http://dx.doi.org/10.5155/eurjchem.5.3.643-469,973>
- Henary et al., 2013 – Henary, M., Levitz, A. (2013). Synthesis and applications of unsymmetrical carbocyanine dyes. *Dyes pigments* 99: 1107-1116. DOI: <https://doi.org/10.1016/j.dyepig.2013.08.001>
- Shindy et al., 2015 – Shindy, H.A., Gomaa, M.M., Harb, N.A. (2015). Synthesis, spectral behavior and biological activity of some novel 1,3,4-oxadiazine cyanine dyes. *Eur. J. Chem.* 6(2): 151-156. DOI: <http://dx.doi.org/10.5155/eurjchem.6.2.151-156.1218>

- Shindy et al., 2016 – Shindy, H.A., Khalafallah, A.K., Goma, M.M., Eed, A.H. (2016). Novel hemicyanine and aza-hemicyanine dyes: synthesis, spectral investigation and antimicrobial evaluation. *Eur. J Mol. Biotechnol.* 13(3): 94-103. DOI: 10.13187/ejmb.10.13187/ejmb.2016.13.94
- Ferreira et al., 2015 – Ferreira, D.P., Conceicao, D.S., Prostota, Y., Santos, P.F., Ferreira, L.F.V. (2015). Fluorescent "rhodamine-like" hemicyanines derived from the 6-(N,N-diethylamino)-1,2,3,4-tetrahydroxanthylum system. *Dyes and Pigments.* 112: 73-80. DOI: <https://doi.org/10.1016/dyepig.2014.06.021>
- Li et al., 2012 – Li, Z., Sun, S., Liu, F., Pang, Y., Fan, J., Song, F., Pang, X. (2012). Large fluorescence enhancement of a hemicyanine by supramolecular interaction with cucurbit[6]Urill and its application as resettable logic gates. *Dyes and Pigments.* 93(1-3): 1401-1407. DOI: 10.1016/j.dyepig.2011.10.005
- Miki et al., 2017 – Miki, K., Kojima, K., Oride, K., Harada, H., Morinibu, A., Ohe, K. (2017). pH-Responsive near-infrared fluorescent cyanine dyes for molecular imaging based on pH sensing. *Chem. Commun.* 53: 7792-7795. DOI: <https://doi.org/10.1039/c7cc03035e>
- Park et al., 2013 – Park, J., Kim, D., Lee, K., Kim, Y. (2013). Reactive cyanine fluorescence dyes indicating pH perturbation of biomolecules. *Bulletin of Kor. Chem. Soc.* 34(1): 1-4. DOI: <https://doi.org/10.5012/bkcs.2013.34.1.287>
- Xiang-Han et al., 2008 – Xiang-Han, Z., Lan-Ying, W., Zhi-Xiang, N., Shi-Huan, T.Z., u-Xun, Z. (2008). Microwave-assisted solvent-free synthesis and spectral properties of some dimethine cyanine dyes as fluorescent dyes for DNA detection. *Dyes and Pigments.* 79: 205-209. DOI: 10.1016/j.dyepig.2008.02.010
- Hilal et al., 2007 – Hilal, H., Taylor, J. (2007). Determination of the stoichiometry of DNA-dye interaction and application to the study of a bis-cyanine dye-DNA complex. *Dyes and Pigments.* 75: 483-490. DOI: <https://doi.org/10.1016/j.dyepig.2006.6.032>
- Sun et al., 2013 – Sun, R., Yan, B., Ge, J., Xu, Q., Li, N., Wu, X., Song, Y., Lu, J. (2013). Third-order nonlinear optical properties of unsymmetric pentamethine cyanine dyes possessing benzoxazolyl and benzothiazolyl groups. *Dyes and Pigments.* 96: 189-195. DOI: <https://doi.org/10.1016/j.dyepig.2012.07.007>
- Sha et al., 2018 – Sha, X.L., Niu, J.Y., Sun, R, Xu, Y.J., Ge, J.F. (2018). Synthesis and optical properties of cyanine dyes with an aromatic azonia skeleton. *Org. Chem.* 5: 555-560. DOI: <https://doi.org/10.1039/C7QO00889A>
- Upadhyayula et al., 2015 – Upadhyayula, S., Nunez, V., Espinoza, E.M., Larsen, J.M., Bao, D., Shi, D., Mac, J.T., Anvari, B., Vullev, V. (2015). Photo induced dynamics of a cyanine dye: parallel pathways of nonradiative deactivation involving multiple excited state twisted transients. *Chem. Sci.* 6: 2237-2251. DOI: 10.1039/c5sc90020d
- Abd El-Aal et al., 2004 – Abd El-Aal, R.M., Koraiem, A.I.M., El-Deen, N.S. (2004). Pyrazolo quinone heterocyclic compounds and metal complex derivatives in the synthesis of cyanine dyes. *Dyes and Pigments.* 63: 301-314. DOI: <http://doi.org/10.1016/j.dyepig.2004.03.008>
- Fayez, 2009 – Fayez M. Eissa (2009). Preparation, antimicrobial activity and absorption spectra of pyrazolo-oxadiazine cyanine dyes. *J. Chin. Chem. Soc.* 56: 843-849. DOI: <https://doi.org/10.1002/jccs.200900125>
- Alessio et al., 2012 – Alessio Raimondi et al. (2012). Electrochemical computational, and photophysical characterization of new luminescent dirheniumpyridazine complexes containing bridging OR or SR anions. *Inorg. Chem.* 51(5): 2966-2975. DOI: 0.1021/ic202284a
- Carlo et al., 2012 – Carlo Ballatore et al. (2012). Amino thienopyridazine inhibitors of tau aggregation: evaluation of structure-activity relationship leads to selection of candidates with desirable in vivo properties. *Bioorg. Med. Chem.* 20(14): 4451-4461. DOI: 10.1016/j.bmc.2012.05.027
- Vijay et al., 2011 – Vijay Chudasama et al. (2011). Bromopyridazinedione-mediated protein and peptide bioconjugation. *Chem. Comm.* 47(31): 8781-85. DOI: 10.1039/C1CC12807H
- Asif, 2012 – Asif, M. (2012). Some recent approaches of biological active substituted pyridazine and phthalazine drugs. *Curr. Med. Chem.* 19(18): 2984-2991. DOI: 102174/09298 671-2800672139
- Siddiqui et al., 2011 – Siddiqui, A., Mishra, R., Husain, A., Rashid, M., Pal, P. (2011). Triazole incorporated pyridazinones as a new class of antihypertensive agents: design, synthesis and in vivo screening. *Bioorg. Med. Chem. Lett.* 21(3): 1023-1026. DOI: 10.1016/j.bmcl.2010.12.028

- Rathish et al., 2012 – Rathish, I., Kalim, J., Shamim, A., Sameena, B., Alam, M., Akhter, M., Pillai, K., Ovais, S., Samim, M. (2012). Synthesis and evaluation of anticancer activity of some novel 6-aryl-2(p-sulfamyl phenyl)-pyridazin-3(2H)-ones. *Eur. J. Med. Chem.* 49: 304-309. DOI: 10.1016/J.ejmech.2012-01.026
- Othman et al., 2014 – Othman, M.M., Nasr, H.M., Hassan, M.I. (2014). Synthesis of some novel pyridazine, thienopyridazine, pyrazolopyridine pyridopyrazolo-pyrimidine and pyridopyrazolotriazine derivatives with their antimicrobial activity. *Can. Chem. T.* 2: 504-517. DOI: 10.13179/Canchemtrans. 2014.02.04.0133
- Ruso et al., 2014 – Ruso, J., Rajendiran, N., Srinivas, C., Murthy, K.N., Soumya, K. (2014). Antimicrobial activities of novel 3-substituted[1,2,4]triazolo[4,3-b]pyridazines derivatives. *J. Kor. Chem. Soc.* 58(4): 377-380. DOI: 10.5012/jkcs.2014.58.4.377
- Asif et al., 2012 – Asif, M., Singh, A., Siddiqui, A. (2012). The effect of pyridazine compounds on the cardio-vascular system. *Med. Chem. Res.* 21: 3336-3346. DOI: 10.1007/S00044-011-9835-6
- Onal et al., 2011 – Onal, Z., Zeng, H., Sonmez, M. (2011). Synthesis, characterization and photoluminescence properties of Cu(II), Co(II), Ni(II) and Zn(II) complexes of N-aminopyrimidine 2-thione. *Turk. J. Chem.* 35: 905-914. DOI: 10.3906/kim1103-55
- Abdalla, 2015 – Abdalla, N.A. (2015). Chelating behavior of dihydrothieno[3,4,d] pyridazine derivatives with some lanthanide and actinide metals. *Chemical Science Transactions.* 4(4): 981-994. DOI: 10.7598/Cst2015.1124
- Ballatore et al., 2012 – Ballatore, C., Crowe, A., Piscitelli, F., James, M. (2012). Amino thienopyridazine inhibitors of tau aggregation: evaluation of structure-activity relationship leads to selection of candidates with desirable in vivo properties. *Bioorg. Med. Chem.* 20: 4451. DOI: <https://doi.org/10.1016/j.bmc.2012.5.027>
- King et al., 2010 – King, P., Lomovskaya, O., Griffith, D., Burns, J., Dudley, M. (2010). In vitro pharmacodynamics of levofloxacin and other aerosolized antibiotics under multiple conditions relevant to chronic pulmonary infection in cystic fibrosis. *Antimicrob. Agents Ch.* 54: 143-148. DOI: 10.1128/AAC.00248-09
- El-Mashad et al., 2012 – El-Mashad, N., Foad, M.F., Soudy, N., Salem, D.A. (2012). Susceptibility tests of oropharyngeal candida albicans from Egyptian patients to fluconazole determined by three methods. *Braz. J. Microbiol.* 43: 266-273. DOI: 10.1590/S1517-83822012001000031
- Mohamed et al., 2014 – Mohamed, M.A., Ibrahim, O.B. (2014). Study the chemical composition and biological outcomes resulting from the interaction of the hormone adrenaline with heavy elements: Infrared, Raman, electronic, ¹H NMR, XRD and SEM studies. *J. Mol. Struct.* 1056: 13-24. DOI: <https://doi.org/10.1016/j.molstruc.201310.019>
- Tarek et al., 2015 – Tarek Aysha, Mervat El-Sedik, Hamada M. Mashaly, Morsy El-Asasery, Oldřich Machalický, Radim Hrdina (2015). Synthesis, characterization, and applications of isoindigo/pechmann dye heteroanalogue hybrid dyes on polyester fabric. *Coloration Technol.* 131: 1-9. DOI: 10.1111/cote.12161
- Tarulata et al., 2011 – Tarulata B. Shah, Ravindran S. Shiny, Ritu B. Dixit, Bharat C. Dixit (2011). Synthesis and dyeing properties of new disazo disperse dyes for polyester and nylon fabrics. *Journal of Saudi Chemical Society:* 1-9. DOI: 10.1016/j.jscs.2011.11.022
- Kubelka et al., 1931 – Kubelka, N.A., Munk, F.Z. (1931). Ein Beitrag Zur Optik Der Farbanstriche. *Tech. Phys.* 12: 593.
- Gomaa et al., 2012 – Gomaa, M.M., El-Deen, N.S., El-Kanzy, N.A. (2012). Benzo[g] quinoline heterocyclic derivative as a typical precursor in the synthesis of new class of cyanine-like dyes. *Eur. J. Chem.* 3(4): 461-467. DOI: 10.5155/eurjchem.3.4.461-467,699
- Ahmed et al., 2018 – Koraiem, A.I., EL-Shafei, A., Abdallah, I.M., Abdel-Latif, F.F., Abd El-Aal, R.M. (2018). Theoretical and experimental spectroscopic investigation of new polymethine donor- π -acceptor cyanine dyes: synthesis, photophysical and TDDFT studies. *J. Mol. Struct.* 1173: 406-416. DOI: <https://doi.org/10.1016/j.molstruc.2018,07.021>
- Shindy et al., 2019 – Shindy, H.A., EL-Maghraby, M.A., Goma, M.M., Harb, N.A. (2019). Polynuclear heterocyclic monomethine and trimethine cyanine dyes: synthesis and various absorption spectra studies. *Eur. J. Mol. Biotechnol.* 7(1): 25-39. DOI: 10.13187/ejmb.2019.1.25

[Shindy et al., 2015](#) – *Shindy, H.A., Khalafallah, A.K., Gomaa, M.M., Eed, A.H.* (2015). Synthesis and photosensitization evaluation of some novel polyheterocyclic cyanine dyes. *Eur. Rev. Chem. Res.* 5(3): 180-188. DOI: 10.13187/ercr.2015.5.180

[Shindy, 2018](#) – *Shindy, H.A.* (2018). Structure and solvent effects on the electronic transitions of some novel furo/pyrazole cyanine dyes. *Dyes Pigments.* 149: 783-788. DOI: <https://doi.org/10.1016/j.dyepig.2017.11.055>

[Shindy et al., 2017](#) – *Shindy, H.A., Khalafallah, A.K., Gomaa, M.M., Eed, A.H.* (2017). Synthesis, spectral sensitization, solvatochromic and halochromic evaluation of new monomethine and trimethine cyanine dyes. *Eur. J. Mol. Biotechnol.* 5(1): 30-42. DOI: 10.13187/ejmb.2017.1.30

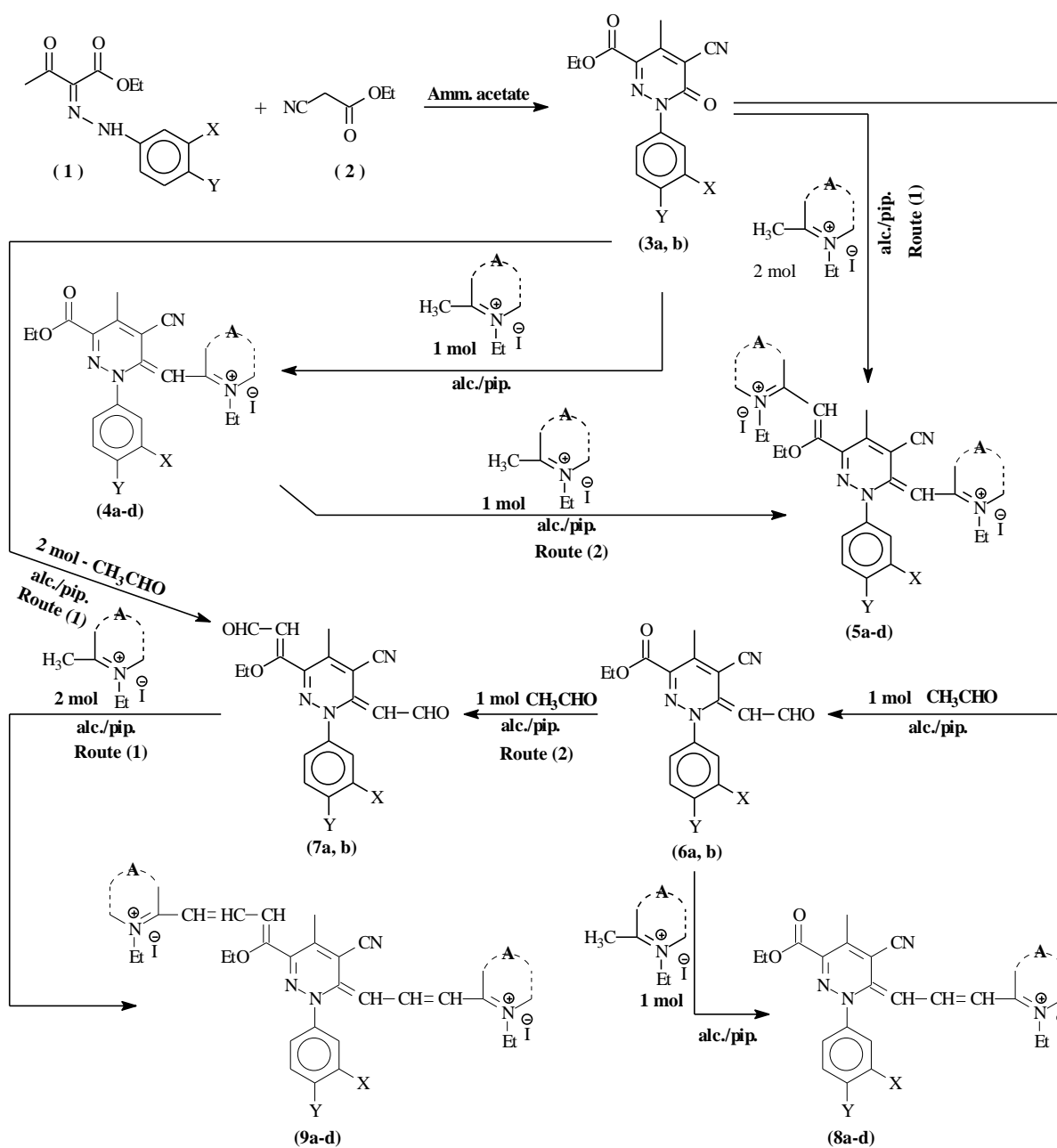
[Shindy et al., 2015](#) – *Shindy, H.A., Gomaa, M.M., Harb, N.A.* (2015). Synthesis, structure/spectra correlation and chromism studies of some novel monomethine and bis-monomethine cyanine dyes. *Eur. Rev. Chem. Res.* 4(2): 126-140. DOI: 10.13187/er-cr.2015.4.126

[Soriano et al., 2016](#) – *Soriano, E., Holder, C., Levitz, A., Henary, M.* (2016). Benzo[c,d]Indolium containing monomethine cyanine dyes: synthesis and photophysical properties. *Molecules.* 21(1): 23-37. DOI: <https://doi.org/10.3390/molecules.21010023>

[Shindy et al., 2018](#) – *Shindy, H.A., El-Maghraby, M.A., Gomaa, M.M., Harb, N.A.* (2018). Synthesis, electronic transitions and antimicrobial activity evaluation of novel monomethine and trimethine cyanine dyes. *Eur. J. Mol. Biotechnol.* 6(2): 83-95. DOI: 10.13187/ejmb.2018.2.83

[Gomaa, 2019](#) – *Gomaa, M.M.* (2019). Novel simple cyanine, carbocyanine, and dicarbocyanine dyes: synthesis, characterization and application on polyester fabric. *Eur. J. Mol. Biotechnol.* 7(2): 73-85. DOI: 10.13187/ejmb.2019.2.73

Appendix 1



Sche

me 1. Synthesis strategy of the prepared compounds (4a-d), (5a-d), (8a-d) and (9a-d)

Substituents in Scheme 1:

(3a, b); (6a, b); (7a, b): X = H, Y = NO₂ (a), X = NH₂, Y = CH₃ (b).

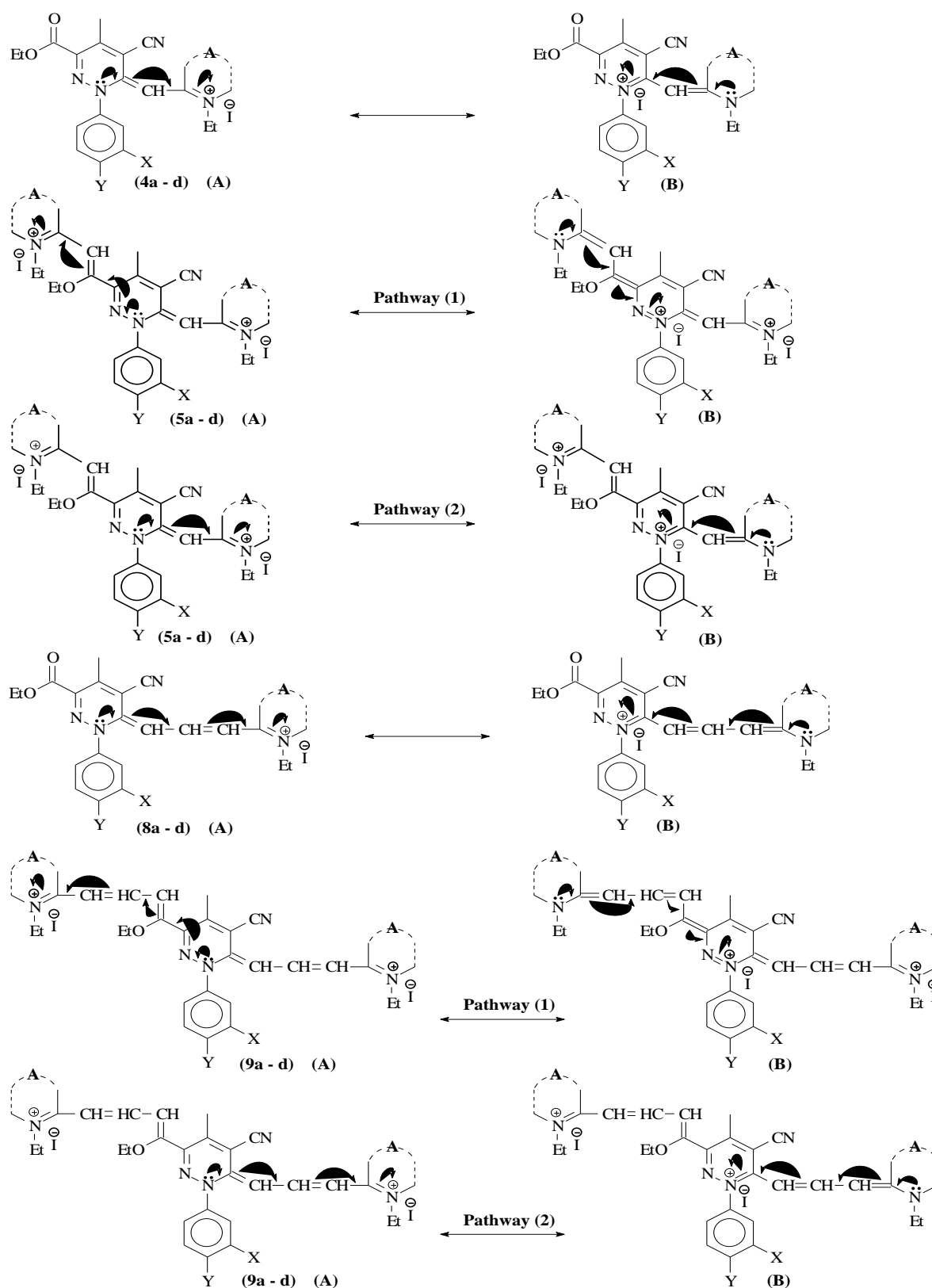
(4a-d); (5a-d); (8a-d); (9a-d): X = H, Y = NO₂, A = 1-ethyl pyridinium 2-yl salt (a);

X = H, Y = NO₂, A = 1-ethyl quinolinium 2-yl salt (b);

X = NH₂, Y = CH₃, A = 1-ethyl pyridinium 2-yl salt (c);

X = NH₂, Y = CH₃, A = 1-ethyl quinolinium 2-yl salt (d).

Appendix 2



Scheme 2. Colour intensity and the charge transfer pathways illustration of the prepared monomethine (4a-d), bismonomethine (5a-d), trimethine (8a-d) and bistrimethine cyanine dyes (9a-d)

Copyright © 2021 by Academic Publishing House Researcher s.r.o.



Published in the Slovak Republic
European Journal of Molecular Biotechnology
Has been issued since 2013.
E-ISSN: 2409-1332
2021. 9(1): 26-30

DOI: 10.13187/ejmb.2021.1.26
www.ejournal8.com



Ligand and ASIC Receptor Interactions in a Rat Ischemic Stroke Model

Elena N. Nesmeyanova ^a, Galina A. Sroslova ^a, Margarita V. Postnova ^a, Nikita V. Panin ^a, Yuliya A. Zimina ^a

^a Volgograd State University, Russian Federation

Abstract

One of the current issues of medicine and pharmacology is investigating the factors that induce cerebral ischemia. In the last few years, there has been a growing interest in the role of ion homeostasis in this disease. However, most previous studies have mainly focused on individual ion channel genes that are responsible for cerebral ischemia development, especially, under adverse conditions. Very little is known about how many ion channel genes are involved in the disease development or its prevention, or whether the changes in different ischemia brain conditions may differ. The most important of these factors is extracellular acidosis. ASIC receptors (voltage-independent proton-gated cation channels) are able to detect physiological changes associated with acid concentration increase. A number of authors consider ASICs to be the most promising target to prevent neuronal injury after ischemic stroke. ASIC activation has an impact on pain sensation, ischemic neuronal injury, neuronal degeneration and mechanosensation that allows ASICs to become potential therapeutic targets for manipulating pain sensations and neurological disorders. In addition to screening for new ASIC1a inhibitors, known ASIC inhibitors can undergo structural modification in order to develop new strong and highly specific inhibitors. Inhibitors of small molecules targeting ASICs may serve as promising therapeutic agents for stroke treatment as well as for psychological adjustment. The paper describes mechanisms of ASIC receptors' activation, localization, and role in physiological processes. A model of ischemic stroke in rats has also been observed.

Keywords: Acid-Sensing Ion Channels (ASIC), acidosis, ischemic stroke, ion channels, Ca²⁺-Permeable Channels.

1. Introduction

For proper functioning, every system of a living organism requires the extracellular environment to be stable, which implies maintenance of an optimal acid-base balance. A process leading to increased acidity in the extracellular environment, termed acidosis, directly affects the nervous system, causing various pathological processes. A decrease in extracellular pH has an impact on cerebral ischemia progression, enhancing it (Chu et al., 2014; Sherwood et al., 2011).

2. Results and discussion

Ischemic stroke is caused by a blockage which interrupts blood flow to the brain (Xiong, 2004). Ischemic stroke contributes to most traumatic brain injuries and remains the common cause of long-term disability and death. Today, there are two ways to treat this disease: liquefaction of blood clots with tissue plasminogen activator (tPA) and endovascular surgery that can be hampered by a number of factors (Kotoda et al., 2017). Recently, new promising candidates for stroke treatment have been discovered. Acid-sensing ion channels (ASICs) are able to predict stroke. However, local decreases in brain pH can cause difficulties that lead to Ca²⁺ excessive overload (Xiong, 2004).

Acid-Sensing Ion Channels are voltage-insensitive cation channels activated by protons and widely spread throughout the central and peripheral nervous systems (1, 9, [Kotoda et al., 2017](#)). ASICs are members of the Degenerin/Epithelial Sodium Channel superfamily (DEG/ENaC/EDA(ASIC)) ([Chu et al., 2014](#); [Hernandez-Encarnacion et al., 2017](#); [Kotoda et al., 2017](#)). Members of this family share the same topology ([Figure 1B](#)) consisting of two hydrophobic transmembrane domains, a large cysteine-rich extracellular loop and short intracellular N- and C-termini ([Hernandez-Encarnacion et al., 2017](#)). ASICs are activated by extracellular pH drop. These ASIC channel subunits are located within the cell bodies and sensory nerve terminals which is important for the processes of nociception and mechanosensing. In central neurons, ASICs are located within the cell bodies, dendrites, and dendritic spines, which is important for synaptic plasticity ([Chu et al., 2014](#)).

In mammals, there are four ASIC genes encoding six different subunits: ASIC1a, ASIC1b, ASIC2a, ASIC2b, ASIC3, and ASIC4 ([Chu et al., 2014](#); [Xiong, 2004](#); [Kotoda et al., 2017](#)).

Each ASIC subunit has a different sensitivity to pH levels that allows these receptors to detect a wide range of physiological pH values. ASIC1 and ASIC3 are sensitive to mild extracellular acidosis whereas ASIC2a is activated in the conditions of lower pH. Each subunit is remarkable for different properties of its kinetics and ionic selectivity ([Hernandez-Encarnacion et al., 2017](#)).

ASIC1a, ASIC2a and ASIC2b channels are commonly located in both the peripheral and central nervous system, whereas ASIC3 and ASIC1b are expressed typically only in the peripheral ([Xiong, 2004](#)). ASICs are also known to be located in some nerve cells such as astrocytes, vascular smooth muscle cells and glioma cells ([Hernandez-Encarnacion et al., 2017](#)). In rats, ASIC3 is specifically concentrated in the sensory neurons. ASIC3 is expressed in sympathetic cardiac afferents innervating the heart, where they may serve as mediators of cardiac pain. As for ASIC2a, its expression in sensory neurons is lower compared to other ASICs. ASIC2a has also been found in the taste buds of the circumvallate papillae, where the receptor may have a function in sour taste perception. ASIC2b has been found only in rats ([Wang, 2013](#)).

A recently resolved crystal structure from chicken (*Gallus gallus*) has demonstrated that ASIC subunits assemble as trimers to form functional channels. They can consist of different subunits, termed heteromeric, or they can consist of identical subunits, termed homomeric ([Xiong, 2004](#); [Chu et al., 2014](#)). The low pH crystal structure of the chicken ASIC1 resembles a bowl-shaped homotrimer with each subunit consisting of short amino and carboxyl termini, two transmembrane helices, and extracellular regions with multiple domains that are enriched with acid residues ([Xiong, 2004](#)).

The location of each ASIC1 subunit may be compared to a forearm and a clenched hand. The extracellular domain consists of a palm (transmembrane domains 1 and 2), a β -ball, a knuckle, a finger, and a thumb. Within the extracellular domain, there is an acidic pocket which is charged highly negatively and is formed by the residues of the palm, the β -ball, the finger, and the thumb. The structure of the transmembrane domain may be compared to an hourglass, with each of the transmembrane domains (TM) defined by two long α -helices. Both TM1 and TM2 consist of three subunits that are related by the three-fold axis of crystallographic symmetry. Most of the TM1 helices' contact is located within the phospholipid bilayer, whereas the TM2 helices line the presumed ion channel pore ([Xiong, 2004](#); [Leng et al., 2014](#)).

ASICs have previously been reported to play a critical role in such physiological processes as nociception, mechanosensation, behavior, fear, and synaptic plasticity. Also, they have a critical role in pathological conditions, such as ischemic stroke, spasm, multiple sclerosis, and tumor cell migration ([Xiong, 2004](#)).

ASICs display a transient proton-activated peak current that lasts from hundreds of milliseconds to seconds, followed by channel desensitization, despite the presence of a solution with low extracellular pH level. The acid-base balance needed for half maximal activation of ASIC currents depends on channel type ([Hernandez-Encarnacion et al., 2017](#)).

ASIC1a homomers commonly expressed in the nervous system have been demonstrated to respond to low pH levels, mediating rapid and transient internal currents with a pH threshold of ~ 7.0 ([Xiong, 2004](#)). Decrease in pH level during ischemic stroke is caused by hypoxia, which intensifies anaerobic glycolysis and in this way contributes to a buildup of lactic acid and the development of acidosis ([Hernandez-Encarnacion et al., 2017](#); [Xiong, 2004](#)). In the conditions of hyperglycemia, pH value may drop to 6.0, whereas it reaches 6.5 at normal blood sugar levels. Such

deviations in pH are sufficient to activate homomeric ASIC1a as well as other brain channels containing ASIC1a. Some functional ASIC1a changes occur during acidosis and oxygen-glucose deprivation, including an increase in current amplitude and a decrease in ASIC desensitization (Xiong, 2004; Chu et al., 2014). These effects potentiate toxic Ca^{2+} loading and may contribute to chronic activation during conditions of brain ischemia (Hernandez-Encarnacion et al., 2017). Moreover, concurrent activation of Ca^{2+} , calmodulin kinase II and N-methyl-D-aspartate (NMDA) contributes to ASIC1a mediated neuronal death. Excessive concentration of intracellular Ca^{2+} may activate a number of enzymes such as phospholipase A2 (PLA2) and nNOS, resulting in excessive generation of reactive oxygen and nitrogen species followed by damage (Xiong, 2004). It proves that acidosis can damage neurons whether or not voltage-gated Ca^{2+} channels and glutamate receptors are activated. Acid-induced neuronal damage may be mitigated by inhibition of ASICs and a decrease in extracellular Ca^{2+} concentration. It has led us to conclude that ASIC channels may serve as new targets for stroke therapy (Kotoda et al., 2017). Today, stroke research may be focused on approaches to limit of ASIC activity and expression.

ASICs have been reported to play an important role in ischemic stroke models (Sherwood et al., 2011; Wang, 2013). In a focal ischemia model, the pharmacological inhibition of the ASIC1a activity or disruption of the ASIC1a gene protects the brain from ischemic injury (Leng, Xiong, 2013; Chassagnon, 2017; Leng et al., 2014; Wu et al., 2013; Simard et al., 2007). It has been demonstrated that agents potentiating ASIC1a activity such as spermine, dynorphin and nitric oxide exacerbate acidosis-mediated neuronal injury and brain ischemia. It has also been shown that increasing surface expression of ASIC1a (e.g., by means of inhibition of ASIC1a internalization) exacerbates acidosis-induced neuronal damage (Leng et al., 2014).

In a mouse model of focal ischemia, the activation of either ASICs or glutamate receptors both contributed to brain injury (Leng et al., 2014). A recent study in a rat cardiac model of global ischemia has shown that amiloride medication inhibiting ASICs and blocking NMDA receptor is able to reduce neurodegeneration (Simard et al., 2007). It might be evidence that, in some brain ischemia models, ASICs have a more important role than NMDA receptors in the mediation of neuronal damage.

The common response of ASIC1a receptors is characterized by a transient inward current. In electrophysiological recordings *in vitro*, the ASIC1a current is usually desensitized within several seconds. Moreover, pre-exposure of ASIC1a with a small decrease of the pH level, which is not sufficient for channel activation, inhibits the channel activation upon followed large pH decreases (Xiong, 2004). These results raise an important question as to what a role the ASIC1a channel activation plays in ischemic brain injury. According to one explanation, endogenous modulators exist and are able to prevent the ASIC desensitization and/or potentiate ASIC responses (Li et al., 2016). At that point, a number of recently-identified endogenous molecules are able to markedly modulate the ASIC properties.

Lactate has the ability to enhance, but not to activate ASIC channels. In addition, it can chelate divalent cations (Zn^{2+} , Ca^{2+} , Mg^{2+} , Cu^{2+} , Ba^{2+} , Pb^{2+} , Cd^{2+} , Ni^{2+} , and Gd^{3+}), modulating ion channels (Hernandez-Encarnacion et al., 2017; Li et al., 2016; Xiong, 2004). Most of the divalent cations listed inhibit ASICs, but only Zn^{2+} has a complex modulatory function on the channels containing ASIC1a and ASIC2a (Xiong, 2004). At physiological concentrations, Zn^{2+} enhances acid activation of homomeric or heteromeric ASIC2a channels, raising the activation dependence on pH up to higher values (Hernandez-Encarnacion et al., 2017).

Arachidonic acid is known to enhance the ASIC activity. Addition of 5 or 10 μM of the acid has led to a significant potentiation of the ASIC current in Purkinje cells from the rat cerebellum. Moreover, arachidonic acid has enhanced or induced a sustained ASIC current. A possible explanation for this phenomenon may be that arachidonic acid potentiates ASICs by stretching the cell membrane upon insertion (Li et al., 2016; Xiong, 2004).

Spermine is known to inhibit desensitization in open-state ASIC1a. However, it accelerates ASIC1a recovery after desensitization in response to repeated acid stimulation (Hernandez-Encarnacion et al., 2017; Li et al., 2016). In addition, ASIC1a activity can be modulated by serine proteases. Protease exposure increases the activity of ASIC1a. Moreover, protease treatment has been proven to accelerate ASIC1a recovery from desensitization (Kellenberger et al., 2015). Calmodulin II (CaMKII), nitric oxide (NO) and dynorphins also play an important role in ischemic injury and ASIC modulation (Hernandez-Encarnacion et al., 2017; Xiong, 2004). ASIC1a and

ASIC2 overlap each other in brain expression (Kotoda et al., 2017). Aside from homomeric ASIC1a, heteromeric ASIC2b/1a is also permeable to Ca^{2+} ions and contributes to neuronal injury induced by acidosis. Homomeric ASIC2b cannot form functional channels, whereas heteromeric ASIC2b/1a is known to produce proton-gated currents (Xiong, 2004).

Among the different ASIC channels, desensitization may vary. E.g., ASIC1 and ASIC3 desensitize faster than ASIC2. Under certain conditions, inactivation of the current carried by some ASIC heteromers is incomplete. It leaves a sustained residual inward current following the fast transient current. This current might be found under the conditions of prolonged acidification in cells that express ASIC3 homomultimers or the heteromers ASIC2a/ASIC2b, ASIC2a/ASIC3, and ASIC2b/ASIC3. Interestingly, the sustained currents in ASIC-expressing cells have different biophysical and pharmacological features from the transient currents. The reasons for these functional differences have not been satisfactorily explained. Transient and sustained currents might involve different types of ASIC channels. It is also possible that sustained currents represent leakage currents due to ASIC overexpression (Hernandez-Encarnacion et al., 2017).

Kinetics of the desensitization changes when ASIC1a subunits are combined with other ASIC subunits, e.g., ASIC2b. When ASIC1a/2b heteromers are combined, the dependence of steady-state desensitization on pH level drops to lower pH values (7.28 for ASIC1a/2b and 7.18 for ASIC1a homomers). The drop in desensitization pH leads to a decrease of ASIC activity after slight decreases in baseline pH. This shift may be neuroprotective in nerve cells or in regions that express a higher amount of ASIC1a/2b heteromers (Kotoda et al., 2017). This has led us to conclude that like homomeric ASIC1a channels, ASIC2b/1a heteromeric channels might contribute to neuronal injury mediated by acidosis. It is also important to note that activation of ASIC2b/1a might result in intercellular Ca^{2+} overload and cell death, which was thought to be mediated only by homomeric ASIC1a (Li et al., 2016; Kotoda et al., 2017). Recently, human ASIC1a channels have been found to have two desensitization states: short- and long-lasting. One of desensitization forms is prevented by high frequency stimulation that somewhat models usage dependent stimulation. Desensitization properties are also determined by the duration of stimulation. However, long term repetitive stimulation results in gradual irreversible loss of channel activity (Kotoda et al., 2017). Having only eight residues distinct from chicken ASIC1a, human ASIC1a has a number of desensitization properties found in chicken, mouse and rat ASIC1a. Surprisingly, the replacement of transmembrane domain 1 (TM1) of hASIC1a has demonstrated the largest effect on the current desensitization compared to individual amino acid mutations.

Homomeric and heteromeric ASICs can be modified by serine proteases such as trypsin, chymotrypsin, and proteinase K (Kellenberger et al., 2015). In addition, endogenous agents can also limit ASIC desensitization. Neuropeptides have recently been found to enhance ASIC1a activity preventing sustained desensitization (Li et al., 2016; Kotoda et al., 2017). Dynorphins are among the basic neuropeptides and they are widely expressed throughout the central nervous system, including areas with high concentration of ASIC1a that are located in stroke-injured regions. Focal accumulation of dynorphin in these regions is suggested to enhance neuronal injury due to increased ASIC activation and subsequent accumulation of Ca^{2+} ions (Kotoda et al., 2017).

ASIC inhibition is often caused by neuroprotective medications. Amiloride is known to be an important pharmacological tool for all known members of the ASIC ion channel family (Kotoda et al., 2017), as it has been previously reported to be able to inhibit ASICs and reduce neurodegeneration (Simard et al., 2007). Amiloride can inhibit all combinations of ASIC subunits (with the exception of the sustained part of ASIC3 current). Intracerebroventricular amiloride injection in mice before transient middle cerebral artery occlusion (MCAO) has been demonstrated to decrease ischemic injury that might be caused by the wide spread of ASIC inhibition (Kotoda et al., 2017). Another research has tested amiloride in a model of a transient ischemic attack caused by middle cerebral artery occlusion (MCAO). A decrease in infarct volume has been observed after intracerebroventricular injection of ASIC1a, amiloride, and PcTx1 blockers (Hernandez-Encarnacion et al., 2017).

3. Conclusion

In summary, ASICs play an important role in cerebral ischemia. ASIC members might become promising pharmaceutical agents for ischemia therapy due to their relatively high

permeability to the blood-brain barrier, the ability to be activated by ligands, and the processes such as mechanotransduction, ion selectivity, or blocking by pharmacological ligands.

ASIC1a can be considered an effective neuroprotective therapeutic target for cerebral ischemia and neuronal degeneration.

4. Conflict of interest

No risk of a conflict of interest.

References

- Chassagnon, 2017 – Chassagnon, I.R. (2017). Potent neuroprotection after stroke afforded by a double-knot spider-venom peptide that inhibits acid-sensing ion channel 1a. *Proc Natl Acad Sci.* 114(14): 3750-3755.
- Chu et al., 2014 – Chu, X.-P., Grasing, K.A., Wang, J.Q. (2014). Acid-Sensing Ion Channels Contribute to Neurotoxicity. *Transl Stroke Res.* 5(1): 69-78.
- Hernandez-Encarnacion et al., 2017 – Hernandez-Encarnacion, L., Sharma, P., Simon, R., Zhou, A. (2017). Condition-specific transcriptional regulation of neuronal ion channel genes in brain ischemia. *Int J Physiol Pathophysiol Pharmacol.* 9(6): 192-201.
- Kellenberger et al., 2015 – Kellenberger, S., Schild, L., Ohlstein, E.H. (2015). International union of basic and clinical pharmacology. XCI. Structure, function, and pharmacology of Acid-sensing ion channels and the epithelial Na⁺ channel. *Pharmacological Reviews.* 67(1): 1-35.
- Kim et al., 2014 – Kim, J.Y., Kawabori, M., Yenari, M.A. (2014). Innate inflammatory responses in stroke: mechanisms and potential therapeutic targets. *Curr Med Chem.* 21(18): 2076-2097.
- Kotoda et al., 2017 – Kotoda, M., Ishiyama, T., Mitsui, K., Hishiyama, S., Matsukawa, T. (2017). Neuroprotective effects of amiodarone in a mouse model of ischemic stroke. *BMC Anesthesiol.* 17(168): 234-241.
- Leng et al., 2014 – Leng, T., Shi, Y., Xiong, Z.-G., Sun, D. (2014). Proton-sensitive cation channels and ion exchangers in ischemic brain injury: new therapeutic targets for stroke? *Prog Neurobiol.* 115: 189-209.
- Leng, Xiong, 2013 – Leng, T.-D., Xiong, Z.-G. (2013). The pharmacology and therapeutic potential of small molecule inhibitors of acid-sensing ion channels in stroke intervention. *Acta Pharmacol Sin.* 34(1): 33-38.
- Li et al., 2016 – Li, M.H., Leng T.-D., Feng X.-C., Yang T., Simon, R.P., Xiong Z.-G. (2016). Modulation of Acid-sensing Ion Channel 1a by Intracellular pH and Its Role in Ischemic Stroke. *J Biol Chem.* 291(35): 18370-18383.
- Radu, 2017 – Radu, R.A. (2017). Etiologic classification of ischemic stroke: Where do we stand? *Clinical Neurology and Neurosurgery.* 159: 93-106.
- Sherwood et al., 2011 – Sherwood, T.W., Lee, K.G., Gormley, M.G., Askwith, C.C. (2011). Heteromeric ASIC channels composed of ASIC2b and ASIC1a display novel channel properties and contribute to acidosis-induced neuronal death. *J Neurosci.* 31(26): 9723-9734.
- Simard et al., 2007 – Simard, J.M., Tarasov, K.V., Gerzanich, V. (2007). Non-selective cation channels, transient receptor potential channels and ischemic stroke. *Biochim Biophys Acta.* 1772(8): 947-957.
- Wang, 2013 – Wang, J. (2013). Does closure of acid-sensing ion channels reduce ischemia/reperfusion injury in the rat brain? *Neural Regen Res.* 8(13): 1169-1179.
- Wu et al., 2013 – Wu, P.Y., Huang, Y.-Y., Chen C.-C., Hsu, T.-T. (2013). Acid-Sensing Ion Channel-1a Is Not Required for Normal Hippocampal LTP and Spatial Memory. *Journal of Neuroscience.* 33(5): 1828-1832.
- Xiong, 2004 – Xiong, Z.G. (2004). Neuroprotection in Ischemia. *Cell.* 118(6): 687-698.

Copyright © 2021 by Academic Publishing House Researcher s.r.o.



Published in the Slovak Republic
 European Journal of Molecular Biotechnology
 Has been issued since 2013.
 E-ISSN: 2409-1332
 2021. 9(1): 31-36

DOI: 10.13187/ejmb.2021.1.31
www.ejournal8.com



Evaluation of Protective Potential of Ethyl Acetate Extract of *Cocus Nucifera* in Gentamycin Induced Nephrotoxicity in Albino Mice

Iboyi Nathaniel Onuche ^{a, *}, Adebayo Joseph Oluwatope ^b

^a Admiralty University of Nigeria, Delta State, Nigeria

^b University of Ilorin, Kwara State, Nigeria

Abstract

Renal disorders have always remained a major area of concern for physicians since a long time and most are of these are drug induced. Antibiotic are used to treat infections caused by organisms that are sensitive to them, e.g gentamycin which is an aminoglycosides which are ototoxic and nephrotoxic. This study looks at the Nephroprotective activity of ethyl acetate extract of husk fibre of *Cocus nucifera* for its protective effects on gentamicin-induced nephrotoxicity in albino mice. For studying acute toxicity study, the study groups contained eight rats in each group and oral dosage of 100, 50, 25 mg ethyl acetate husk fibre of *Cocus nucifera* extract/kg body weights was administered to albino mice. Nephrotoxicity was induced in albino mice by daily intraperitoneal administration of gentamicin 45 mg/kg/day for 10 days. Effect of concurrent administration of ethyl acetate extract of *Cocus nucifera* at a dose of 100, 50 and 25 mg/kg/day given by oral route for 17 days. The biochemical parameter such as serum electrolytes as indicators of kidney damage was determined by using one way ANOVA the results are significant at $P > 0.05$. The result shows that at higher concentration of the extract, kidney damage was not seen while lower concentration it was seen.

Keywords: nephrotoxicity, *Cocus nucifera*, gentamycin, Kidney, Protective, Wistar albino mice, polyphenols, husk fibre, Coconut and ethyl acetate.

1. Introduction

Nephrotoxicity is one of the most common kidney problems and occurs when body is exposed to a drug or toxin. When kidney damage occurs, the body unable to rid of excess urine and wastes from the body and blood electrolytes (such as potassium and magnesium) will all become elevated and Sodium will reduce. A number of therapeutic agents can adversely affect the kidney resulting in acute renal failure, chronic intestinal nephritis and nephritic syndrome because increasing number of potent therapeutic drugs like aminoglycoside antibiotics, chemotherapeutic agents and NSAIDs have been added to the therapeutic arsenal in recent years. Exposure to chemical reagents like ethylene glycol, carbon tetra chloride, sodium oxalate and heavy metals like lead, mercury, arsenic and cadmium also induces nephrotoxicity (Ramya, 2011).

Many plants have been used for the treatment of kidney failure in traditional system of medicine throughout the world. Indeed along with the dietary measures, plant preparation formed the basis of the treatment of the disease until the introduction of allopathic medicine. Traditional knowledge will serve as a powerful search engine and most importantly, will greatly facilitate intentional, focused and safe natural products research to rediscover the drug discovery process.

* Corresponding author

E-mail addresses: nathanieliboyi6@gmail.com (I. Nathaniel Onuche)

Therefore, search of nephroprotective herbs from medicinal plants has become important and need of the day (Bharti et al., 2012).

Nephroprotective agents are the substances which possess protective activity against nephrotoxicity. Medicinal plants have curative properties due to the presence of various complex chemical substances. Ancient literature has prescribed various herbs for the cure of kidney disease (Chan, Elevitch, 2006).

Coconut tree has been eulogised as 'Kalpavriksha' (the all giving tree) in Indian classics for its all round usefulness (Adebayo et al., 2013), Husk fibre of a coconut tree has been reported to have antibacterial, antifungal, antiviral, antiparasitic, antidermatophytic, antioxidant, hypoglycemic, hepatoprotective, immunostimulant, antibleorrhagic, antibronchitis, febrifugal, and antigingivitic properties (Adebayo et al., 2013), and antimalarial activity (Terri, Sesin, 1958). Very few studies were reported in literature regarding histopathology of gentamicin induced renal failure in Albino mice. So, the present study is taken up to see the effect of ethyl acetate extract of *Cocos nucifera*, its nephroprotective properties by investigating the biochemical and histopathological changes of mice.

2. Materials and methods

Wistar albino mice weighing 20-26 g, are utilized for the present study. Experiments were performed with the permission of the institutional ethics committee. In the present study, albino mice were used and are grouped as follows:

Group A: (Control Positive): Administered appropriate volume of 5 % DMSO solution.

Group B: (Control Negative): Administered appropriate volume of 5 % DMSO solution + 200µl Gentamycin.

Group C: Administered 100mg/Kg body weight of *Cocos nucifera* extract fraction + 200 µl Gentamycin.

Group D: Administered 50mg/Kg body weight of *Cocos nucifera* extract fraction + 200 µl Gentamycin.

Group E: Administered 25 mg/Kg body weight of *Cocos nucifera* extract fraction + 200 µl Gentamycin.

Method

All rats were kept under observation for 2 week prior to the experiments to acclimatize with environment. All animals were fed standard rat chow and were provided tap water to drink *ad libitum*. They were housed in a facility with 12-12 h light-dark cycle that is maintained at 25°C. All animals were weighed before the injections. The animals were anaesthetized with diethyl ether inhalation. Blood samples were collected with cardiac puncture for biochemical investigations (serum) Na, K, Cl and HCO₃ were determined, the effect of body ratio and the Histological analysis

Administration of the sample: daily intraperitoneal injection of gentamycin was given to each group for 10 days and the daily oral administration of ethyl acetate extract of *Cocos nucifera* are given to each group for 17 days.

Collection of Blood Sample: At the end of the 17-day experimental period, the Mice were sacrificed by slight diethyl ether anaesthesia, the neck area was quickly cleared of fur and the jugular veins exposed, from which blood was collected into EDTA bottle to prevent clotting. The EDTA blood sample was centrifuged at 3000 rpm for 10 minutes and the serum pipetted out. This was stored frozen at -20°C until needed for analysis.

Determination of serum electrolytes:-Sodium (Na) and Potassium (K) analysis were carried out using Randox Laboratory kit according to the method of Terri et al 1958 (Garetz, Schacht, 1996). Serum calcium was determined colorimetrically using commercial kits (Erba, Germany) according to the method of Moorehead W R et al 1974 (Baliga et al., 1997).

3. Results

Effect of polyphenols of Ethyl Acetate Extract of *Cocos nucifera* Husk Fibre on kidney/Body Weight Ratio

Gentamicin caused a significant increase ($p < 0.05$) in kidney/body weight ratio compared to control (Table 1). The administration of polyphenols of ethyl acetate extract of *Cocos nucifera* husk fibre (WAT) at various doses investigated in this study was not able to reverse the significant increase ($p < 0.05$) in kidney/body weight ratio caused by gentamicin (Table 1).

Table 1. Effect of polyphenols of *Cocos nucifera* Husk Fibre (WAT) on kidney-Body Weight Ratio of mice with gentamicin-induced kidney damage

Treatment (mg/Kg body weight)	Organ Body Weight (%)
Control (5 % DMSO)	0.98±.016 ^a
Gentamicin	1.34±0.08 ^b
Gentamicin + 25mg/kg body weight of polyphenols	1.15±0.09 ^{ab}
Gentamicin + 50 mg/kg body weight of polyphenols	1.27±0.06 ^b
Gentamicin + 100mg/kg body weight of polyphenols	1.33±0.07 ^b

Values are expressed as mean of 5 replicates ± SEM. Values with the same superscript are not significantly different at $p < 0.05$.

Table 2. Effect of polyphenols extract of *Cocos nucifera* husk fibre (WAT) on some selected electrolytes of Gentamycin induced renal impairment in Mice

Group	Na ⁺ (Meq/L)	K ⁺ (Meq/L)	Cl ⁻	HCO ₃
Control (5 % DMSO)	156.08±4.42 ^a	4.50±0.33 ^a	91.25±2.5 ^b	26.15±1.62 ^a
Gentamycin	147.85±2.64 ^b	7.50±0.32 ^b	82.00±6.58 ^b	23.02±2.33 ^a
Gentamycin + 25mg/kg body weight of extract	151.05±0.78 ^a	5.37±0.21 ^a	78.00±5.59 ^a	24.45±1.67 ^a
Gentamycin + 50mg/kg body weight of extract	147.95±4.09 ^a	5.40±0.23 ^a	90.00±3.92 ^b	22.00±1.22 ^a
Gentamycin + 100mg/kg body weight of extract	153.25±5.47 ^a	5.68±0.32 ^a	95.00±3.74 ^b	20.95±1.34 ^a

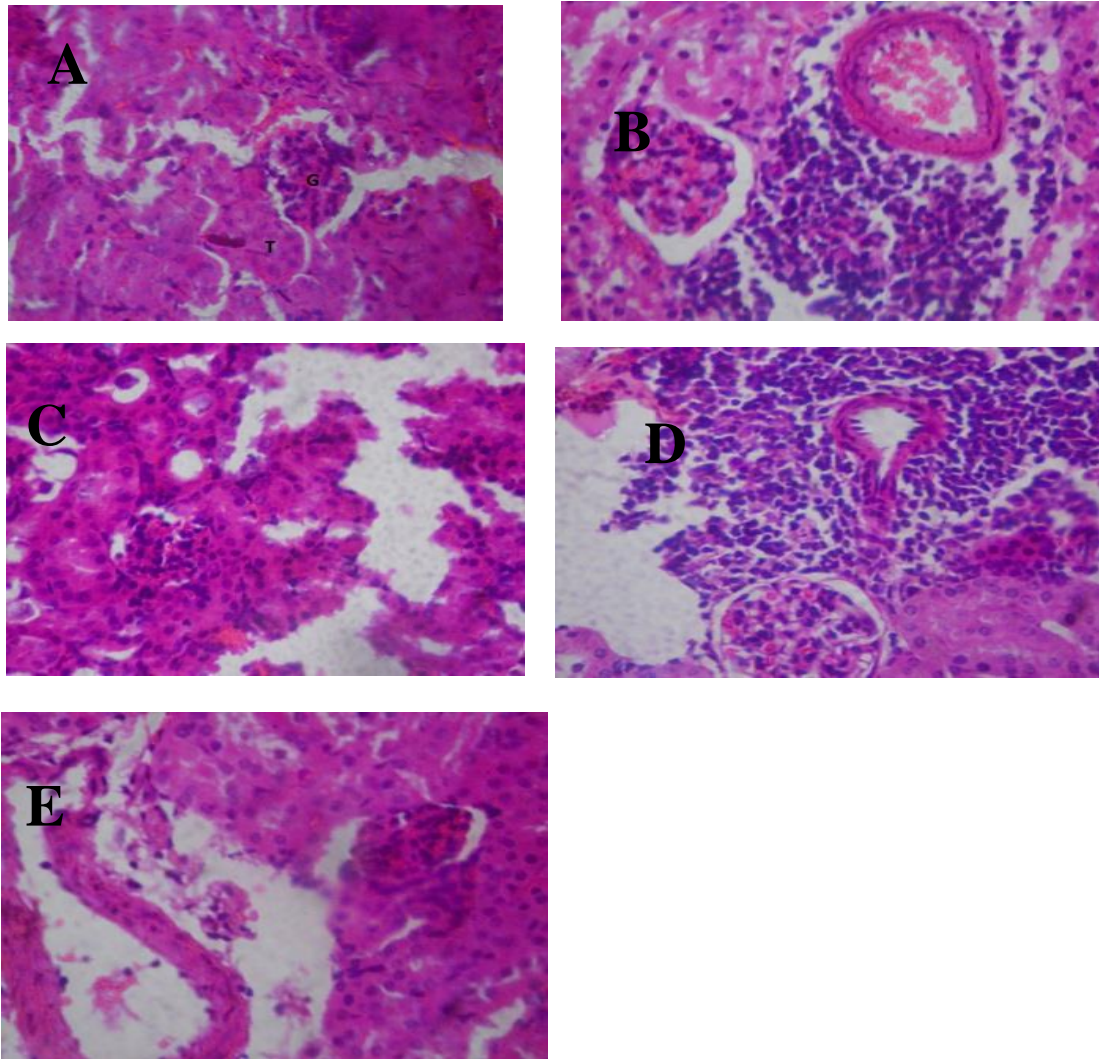
Data are mean ±SEM of five determinations. Values with the same superscript are not significantly different at $p < 0.05$

Protective Effect of polyphenols extract of *Cocos nucifera* husk fibre (WAT) on Histology of kidney of Gentamycin induced renal impairment Mice

Histological analysis revealed that the histo-architectural changes of the kidneys of all the treated animals and the glomerulus Corpuscles reveals the obliteration of the bowman space by the gentamycin (Figure 1).

4. Discussion

The incidence of renal dysfunction following amino-glycoside administration was detected by many workers Garetz and Schacht, 1996; Baliga et al., 1997 and Abdel Naim et al., 1999 (Abdel-Naim et al., 1999; Heibashy et al., 2009; Baliga et al., 1997). The administration of gentamycin into mice induced impairment of renal function through liberation of oxygen free radical (Heibashy, Abdel Moneim, 1999 and Heibashy et al., 2009). Renal failure is characterized by disorders in some biochemical parameters and Kidney function indices. It can be seen that gentamycin produce Nephrotoxicity in the mice by seen the increase in Potassium and lowering the Sodium. Renal function tests are required either to demonstrate the presence or absence of active lesion in the kidney, or to assess the normal functioning capacity of different parts of nephron (Panda, 1989).



Representative photomicrographs of the kidney of albino mice, following administration of varied dosages of polyphenols of *Cocos nucifera* Husk fibre (H&E $\times 100$). A served as control and received DMSO. B received polyphenols and gentamicin while C, D, and E were the experimental groups which received 25 mg/kg, 50 and 100 mg/kg body weights of polyphenols for 17 days and gentamicin for 7 days

Fig. 1. Histological observation of the kidney

Organ-body weight ratios are normally investigated to determine whether the size of the organ has changed in relation to the weight of the whole animal and high Organ to body weight ratio has been associated with inflammation while otherwise is constriction (Ali et al., 2003). The increase in kidney/body weight ratio caused by gentamicin (an aminoglycoside) in this study suggests inflammation. Aminoglycosides have been reported to cause nephrotoxicity through oxidative stress and forming free radicals (Goto, 2004). However, the polyphenols at all doses used in this study were not able to prevent the observed inflammation in the kidney, suggesting that doses used were not sufficient enough to mop up the free radicals generated by gentamicin.

These results confirmed that gentamicin produced nephrotoxicity as previously reported by Ali et al., 2003, Goto, 2004 and Heibashy et al., 2009. Serum electrolytes were disturbed in gentamicin treated mice as compared with control animals and the ethyl acetate of *Cocos nucifera* extract was seen to be able to attenuate this trend by trying to correct the damages done. Those group that receive 100 and 50 mg/kg b.wt of the extract are found to be doing well and the

effectiveness of the extract was seen while those that receive the 25 mg/kg b.wt, the renal function was seen to be serious in them.

Lower value of serum sodium indicated inability of kidney to conserve sodium and chloride. Haemodilution too may be involved in the fall of sodium value via excess of water intake and or increased production of endogenous water. Increase of Potassium may be due to reduced excretion of K aggravated by leakage of intracellular potassium into blood stream as a result of gentamicin induced lesions in renal tubular epithelium. The present results are in harmony with the data obtained by [Heibashy, Abdel Moneim, 1999](#) and [Heibashy et al., 2009](#).

Apoptosis plays a major role in kidney embryogenesis, resulting in large-scale cell death during development. By contrast, in the adult and under normal circumstances, evidence of apoptosis is seldom found in the kidney, where the rate of cell turnover is very low. However, there are a number of documented cases related to kidney insult in both pathology and toxicology where the renal tissue, in particular the tubular epithelium, exhibits a substantial increase of apoptotic cells ([Conaldi et al., 1998](#)).

These results confirmed that gentamicin produced nephrotoxicity as previously reported by [Ali et al., 2003](#), [Goto, 2004](#) and [Heibashy et al., 2009](#). These changes reflected the severity of renal insufficiency which occurred in association with the sudden fall in glomerular filtration rate because of the majority of administrated gentamicin enters specifically the proximal tubular epithelial cells, binds to anionic phospholipids in the target cells inducing abnormalities in the function and metabolism of multiple intracellular membranes and organelles then developed injury in the proximal tubular epithelial cells of kidney that caused acute renal failure. More than half of proximal tubules showing desquamation of necrosis but involved tubules easily found, complete or almost complete tubular necrosis. The polyphenols administered were able to prevent the observed architectural structure of the kidney at dose dependant manner though perivascular inflammations were seen in group B and D.

5. Conclusion

Daily administration of ethyl acetate extract of *Cocus nucifera* for 17days was seen to be able to attenuate the renal dysfunction cause by daily intraperitoneal injection of gentamicin 45 mg/kg b.w for 10 days is evident on renal function tests. Thus, it could be suggested that gentamicin must be given in the lowest effective therapeutic doses in patients with normal kidney function. Also, gentamicin therapy should be preceded by antioxidant administration and also it could be suggested that the husk fibre of ethyl acetate extract of *Cocus nucifera* can be modified into drug so that it can be given before administration of gentamycin because it is seen from this presence studies that it has nephroprotective properties

6. Acknowledgements

I really appreciate Dr. Adebayo, who took his time to go through this piece of work, also to the Professors and all the staff of the Department of Biochemistry, University of Ilorin, Kwara State, Nigeria.

References

- [Abdel-Naim et al., 1999](#) – *Abdel-Naim, A.B., Abdel-Wahab, M.H., Attia, F.F.* (1999). Protective effects of vitamin e and probucol against Gentamicin nephrotoxicity in rats. *Pharmacol Res.* 40(2): 183-187.
- [Adebayo et al., 2003](#) – *Adebayo, J.O., Yakubu, M.T., Egwin, C.E., Owoyele, B.V. Enaibe, B.U.* (2003). Effect of ethanolic extract of *Khaya senegalensis* on some biochemical parameters of rat kidney. *Journal of Ethnopharmacology.* 88: 69-72.
- [Adebayo et al., 2013](#) – *Adebayo, J.O, Balogun, E.A., Malomo, S.O., Soladoye, A.O., Olatunji, L.A., Kolawole, O.M., Oguntoye, O.S., Babatunde, A.S., Akinola, O.B., Aguiar, A.C.C., Andrade, I.M., Souza, N.B., Krettli, A.U.* (2013). Antimalarial Activity of *Cocos nucifera* Husk Fibre: Further Studies. *Hindawi Publishing Corporation, Evidence-Based Complementary and Alternative Medicine.* Article ID 742476.
- [Ali et al., 2003](#) – *Ali, B.H., Al-Qarawi, A.A., Haroun, E.M., Mousa, H.M.* (2003) The effect of treatment with gum arabic on gentamicin nephrotoxicity in rats. *Ren Fail.* 25(1): 15-20.

Baliga et al., 1997 – Baliga, R., Ueda, N., Walker, P.D., Shah, S.V. (1997). Oxidant mechanisms in toxic acute renal failure *Am. J. Kidney. Dis.* 29: 465-477.

Bharti et al., 2012 – Bharti, D., Raghunath. T., Manoj Kumar, Z., Namrata, V. (2012). Nephroprotective plants: A review. *International Journal of Pharmacy and Pharmaceutical Sciences.* 4(1): 8-16.

Chan, Elevitch, 2006 – Chan, E., Elevitch, C.R. (2006). *Cocos nucifera* (coconut), Species Profiles for Pacific Island Agroforestry. *Permanent Agriculture Resources (PAR). Hōhualoa, Hawaii.* 2(1): 127.

Conaldi et al., 1998 – Conaldi, P.G., Biancone, L., Bottelli, A., Wade-Evans, A., Racusen, L.C., Boccellino, M., Toniolo, A. (1998) HIV-1 kills renal tubular epithelial cells in vitro by triggering an apoptotic pathway involving caspase activation and Fas upregulation. *J Clin Investig.* 102: 2041-2049.

Garetz, Schacht, 1996 – Garetz, S.L., Schacht, J. (1996). Ototoxicity of mice and men" In Handbook of auditory research, ed. By R.R. Fay and A.N. Popper, Vol. VII: Clinical aspect of hearing, ed. By T.R. Van De Water, A. N. Popper and R.R. Fay, PP. 116-154, Springer New York.

Goto, 2004 – Goto, A.M. (2004). The role of lipid coronary heart disease. Kalamazoo, M. I. Upjhion Company.

Heibashy et al., 2009 – Heibashy, M.I.A., El-Nahla, A.M., Ibrahim, A.I., Saleh, Sh.Y.A. (2009). Comparative study between dimethyl sulfoxide (DMSO), allopurinol and urate oxidase administration in nephrotoxic rats induced with gentamicin. 43rd Annual Veterinary Medical Symposium, College of Veterinary Medicine Nursing and Allied Health, Tuskegee University, Alabama, USA.

Heibashy, Abdel Moneim, 1999 – Heibashy, M.I.A., Abdel Moneim, A.E. (1999). Kidney and liver function tests after late Dimethyl sulfoxide (DMSO) administration in rats with gentamicin induced acute renal failure. *J. Egypt. Ger. Soc. Zool.* 30(A): 35-48.

Moorehead, Briggs, 1974 – Moorehead, W.R., Briggs, H.C. (1974). Clinical chemistry. 20: 1458.

Ramya, 2011 – Ramya, P. (2011). Nephroprotective medicinal plants – A review. *International Journal of Universal Pharmacy and Life Sciences.* 1(2): 266-281.

Sundin et al., 2001 – Sundin, D.P., Sandoval, R., Molitoris, B.A. (2001). Gentamicin Inhibits Renal Protein and Phospholipid Metabolism in Rats: Implications Involving Intracellular Trafficking. *J Am Soc Nephrol.* 12: 114-123.

Swan, 1997 – Swan, S.K. (1997). Aminoglycoside nephrotoxicity: review. *Seminars in nephrology.* 17(1): 27-33.

Terri, Sesin, 1958 – Terri, A.E., Sesin, P.G. (1958). A.M.G. Clinical Pathology. 29: 86-89.

Copyright © 2021 by Academic Publishing House Researcher s.r.o.



Published in the Slovak Republic
European Journal of Molecular Biotechnology
Has been issued since 2013.
E-ISSN: 2409-1332
2021. 9(1): 37-49

DOI: 10.13187/ejmb.2021.1.37
www.ejournal8.com



Insight into the Natural and Synthetic Factors Responsible for Cell Regeneration in Various Organs

Swayambhik Mukherjee ^{a, *}, Sanchari Das ^b, Shweta Kumari Rowlo ^c, Advait Pk ^d

^a St Xavier's College (Autonomous), Kolkata, India

^b University of Engineering and Management, Kolkata, India

^c SRM University, Chennai, India

^d Annamalai University, Chidambaram, Tamil Nadu, India

Abstract

Cell Regeneration is the key phenomenon liable for the smooth and healthy functioning of our body as it is responsible for replacing the damaged or aged cells. The research focusses on the factors and possible accelerators responsible for cell regeneration, both Natural and Synthetic. In this regard, we have studied the process of cell regeneration closely in individual organs like the bones, heart, skin, eyes, and liver. Our main research question revolves around the reasons that influence the resurgence of cells and also elements that fasten the process. The research highlights various biological events including involvement of growth factors and scientifically implemented techniques like biomodelled chemical substitutes and 3Dbioprinting that have been interpreted to be linked with the renewal of cells in our research.

The research efforts carried out in this article aims to further facilitate the Research and Development (R&D) initiatives of Jozbiz Technologies Pvt Ltd.

Keywords: hexagonal hydroxyapatite (HA), growth factors (GF), opacification.

1. Introduction

A saying goes like no life can proceed without regeneration and no death can ever occur if everything in this universe is regenerated. These are the two extremes between which all organisms seem to exist. The process of reproduction can be otherwise called as regeneration of organisms producing their own species. In this universe each and every organism regenerate.

Regeneration can be subcategorized into several kinds and one of the major one is reproduction specially focusing on the vegetative one. All organisms in this universe have the ability to synthesize molecules to generate additional units of any structure. There is a constant biochemical turnover allowing the additional units to adapt with their physiological changes as they continue to exist. These additional units should continue to multiply in

* Corresponding author

E-mail addresses: swayambhik99@gmail.com (S. Mukherjee), sanchari.d0906@gmail.com (S. Das), sr3376@srmist.edu.in (S. KumariRowlo), advaitpk10@gmail.com (A. Pk)

order to successfully carry out the process of regeneration. The cells should unite together to form tissues which further forms tissues and finally end up forming organs.

Several organs found in various organism are often found to have the capability to regenerate naturally.

It is defined as the process of incorporating or merging man-made or synthetic material into a human for replacing natural tissues or organs. The primary function of this organ regeneration is restoring a particular function or a set of relevant functions providing the patient with a normal life. However, the process is still not fully understood. Even though it consists of tremendous therapeutical capability for humans. In this review paper, we chose to compile or outline the repair and regenerative capability of the organs such as: eyes, liver, skin, bone and cardiac tissues of humans and other organisms. In course of years, organ regeneration has evolved to be an encouraging and hopeful therapy that can cure diseases in humans and other organisms that cannot be healed by other methods or treatment procedures. It also achieved a superior post when compared to any other treatment utilizing exogenous sources in order to substitute the function and/or the structure of the organs that have been lost.

2. Results and discussion

Involvement of Biomodelled chemical substitutes in regeneration of the bone tissue:

Bone tissue encompasses a mineralized construction. Biomimetic composite substitute with a mineral constituent were used loosely for bone repair. The mineral element introduces structural integrity and osteoconductive features to the scaffold. Hexagonal hydroxyapatite (HA) is often used for the rationale that has the potential to simulate the natural minerals a part of bone. Besides, alternative inorganic phosphate such as calcium phosphate or bioglass were equally used because of their biocompatibility. Utilizing dioxane/water as a solvent, nano-HA/poly-l-lactide (PLLA) nanofibers composite scaffolds through TIPS (thermally iatrogenic section separation) technique were invented. The high expanse of the nanofibrous permits more the HA to be exposed, that is suitable for bone tissue regeneration.

In another study, HA was incorporated into electrospun nanofibers, then used a gelatin-apatite precipitate homogenized in Associate in Nursing organic solvent with polylactide-co-caprolactone (PLCL). For the length of the precipitation reaction, the Ca/P proportion was reserved to 1.67 to ensure ratio mineral fabrication. Simply rock bottom concentration of gelatin-apatite ends up in a growth in traditional strength. Lately, deposition methodology has been developed that decreases the mineralization time. To demonstrate the pliability of the technique, deposition has been effectively created on each electrospun PLLA fibers and phase-separated PLLA fibers. As a result, electrodeposition was confirmed to be a quick and operative methodology of mineralization of bone tissue scaffold. Collagen, within the style of injectable hydrogels, membranes, or sponges, extensively used for bone tissue regeneration. singly, as composite with inorganic phosphate structures like HA; many instances embody, collagen/HA/chitosan or collagen/HA/alginate hydrogels ([Ansari, 2019](#)).

Usage of 3DBioprinting in bone tissue regeneration:

3D printing employs 3D pictures of the bone trauma anatomy, sometimes noninheritable from computerized tomography (CT) scans, employing a hard software system, to fabricate a bone graft substitutes (BGS) structure that matches to a bony defect. The personalised bone graft substitute kind employs a 3D printer to regulate the BGS mechanical options and substantial values. The composition optimisation ensures related improved correspondence among the BGS and the patient's anatomy, allowing the regeneration. Replacements factory-made by titanium are very instrumental and most widely used. Metal plates are sometimes used to immobilize bone elements in jaw

operations. 3D printing is equally being studied for orthopaedic purposes: for cotyloid ruptures, mortise joint defects and more bone defects because of bone fracture, spurt fissure of spine, bone cancer and orbital ground repair. The tailored soft/spongy implant printed by Ti6Al4V bestowed outstanding chemical science options and characterized biological performances of biocompatibility, osteogenic property, and bone regeneration. Bioceramics and biopolymers like polyetheretherketone (PEEK) are presently being devised in suitability to usage, and being studied at the pre-clinical stage. Research is being conducted on BMP-2-loaded polycaprolactone(PCL) /HA composite for the repair of animal tissue recession associated with bone and animal tissue tissue repair.

In a recent study, ([Ansari, 2019](#)) a mandibular bone bone was repaired via human amniotic fluid-derived somatic cell (hAFSC)-loaded hydrogel, a combination of PCL and tricalcium phosphate (TCP), and pluronicF12. The PCL/TCP and hAFSCs mixed with the colloidal solution of hydrogel, were reproduced during a kind I style with a PluronicF127 impermanent support . After induction of osteogenic differentiation for twenty eight days, the constructions with alizarin carmine S were stained; staining at the surface of the 3D bone constructions showed metallic element deposition within the hAFSC loaded hydrogel.

Cardiac tissue regenerative apparatus implemented by Growth Factors:

Angiogenesis is the phenomenon of generation of new blood vessels through differentiation of endothelial cells. From the medical purpose, the target is to stimulate vessel growth in patients with conditions characterised by lean blood flow, like anaemia heart diseases and peripheral vascular structure diseases.

As regards the latter side, the identification of growth factors that induce the angiogenic method aroused the interest within the use of those proteins for the induction of therapeutic ontogeny. Within the case of MI, angiogenic medical care with growth factors might salvage the anaemia tissue at early stages of infarct, by provision the tissue with new vessels. This method is crucial to forestall cardiopathy through the management of cardiomyocyte hypertrophy and ability. In fact, ontogeny is that the main growth factor-induced reparative mechanism and has been the mechanism most frequently investigated in experimental studies and clinical trials on slashed heart muscle repair. Most of those studies have dedicated their efforts toward the angiogenic and regenerative potential of vascular structure epithelial tissue protein (VEGF) and embryonic cell protein (FGF).

Mitigation of the anaemia injury within the internal organ tissue is also induced by antiapoptoticfactors, that exert doubtless cardioprotective effects. Hepatocyte protein (HGF) was initial known as a hepatocyte agent, with chemotactic and antiapoptotic actions in numerous cell sorts. In rats undergoing anemia and reperfusion, blood vessel administration of HGF reduced caspase-mediated cell death in cardiomyocytes and therefore the infarction size. Alternative antiapoptotic factors with therapeutic potential in internal organ regeneration embody platelet-derived protein (PDGF-BB) and supermolecule hormone hormone, IL-11, IL-33, and others ([Rebouças et al., 2016](#)).

Endogenous mechanisms mediate by progenitors and stem cells embody mobilization and orienting of bone marrow progenitors also as CSC activation. These cells might differentiate into new cardiomyocytes once the anaemia injury, however their range is reduced or they're insufficiently activated to provide important muscular regeneration. Some proteins show the potential to mobilize bone marrow progenitors to the internal organ lesion space or activate CSC. These properties is also therapeutically explored as regenerative mechanisms activated by growth factors or recombinant proteins, like the white cell colony stimulating issue (G-CSF), HGF, stromal cell-derived issue (SDF-1), and others. The paradigm of the guts as a very differentiated organ was contested supported the identification of mitogens able to induce adult cardiomyocytes to enter into the cell cycle. This method opens the likelihood to stimulate a brand new regeneration mechanism within the infarcted heart, resulting in the formation of a population of recent

cardiomyocytes capable of replacement the cell mass lost because of the anaemia injury. 3 living thing factors are known for his or her ability to activate receptors concerned in cardiomyocyte proliferation: acidic embryonic cell protein (FGF-1), neuregulin (NRG-1), and periostin. Treatment of infarcted rats with FGF-1 together with a mitogen-activating supermolecule enzyme (MAPK) p38 resulted in redoubled cardiomyocyte cell division and improved internal organ operation. Studies have incontestible improved internal organ operate in infarcted mice treated with daily injections of NRG-1.

Table 1. Mechanism of Growth Factor directed Cardiac tissue regeneration

Factor	Effects	Factor	Effects
VEGF	Formation of blood vessels	G-CSF	Prevention of cell death
FGF	Formation of blood vessels	Intermedin	Formation of blood vessels
HGF	Prevention of cell death	Angipoietin	Formation and stabilization of blood vessels
SDF-1	Hematopoietic stem cells orientation	Periostin	Increase in Cardiomyocytes
IGF-1	Stem cells'and antecedent cells' surviving ability and differentiation	Neuregulin-1	Increase in Cardiomyocytes
PDGF	Prevention of cell death	Erythropoietin	Prevention of cell death

Insight into Resurgence of skin cells:

The skin acts as a shield for the internal environment from the external one but in case of damaged or injured epidermis, it is able to thereafter regenerate due of the presence of stem cells. The skin is basically made up of three layers, starting with the uppermost and outermost layer is the epidermis, followed by the dermis which is made up of 95 % keratinocytes, further consisting of five layers, ranging from stratum basale to the stratum corneum. Then comes the layer next to the epidermis, the dermis, made up of connective tissue, hair follicles, and sweat glands followed by hypodermis, which is the is the deepest surface of the skin featuring loose connective tissue.

Keratinocytes are formed by basal cells at the basal cell layer as they migrate to the upper epidermal layers to form a dead cell on the surface of the skin which overtime shed away.

Growth factors, cytokines, chemokines, and other required cells coordinate in order to heal a normal wound, but a deeper or more severe injury might not be healed by the skin because of how complex and multiphase the whole process of cell regeneration is and ends up becoming a chronic injury which may further leave scars (Blanpain, 2010). Treating the chronic injuries requires continuous analysis and repetitive treatment and if left unattended or untreated can lead to much more severe infections. Thus, different strategies of stem-cell therapy have been proposed which have a potential to treat deeper injuries effectively and efficiently. Out of many solutions to heal these kind of skin damages, use of foreign compatible tissue is also one but depends highly on a healthy donor but also contains a lot of risks. According to researches, skin was the very first organ to be engineered that could be used for a patient. Since, tissue engineering and stem cell therapies are an evolving field, over the decade there has been numerous levels of

development and is still continuing to develop. Newer and advanced techniques are able to modify substitutes that hold the potential for a better testing.

Regenerative medicine is a field of medicine that focuses on finding ways to regenerate, repair, or replace cells, organs, and tissues that have been damaged. The synthesis and use of therapeutic stem cells, tissue engineering, and the creation of artificial organs are all examples of regenerative medicine.

According to studies (Martin, 1997) wound healing has been seen in foetal skin and appendages regeneration has been seen in adult skin. The models following this principle has taken this as a potential basis for further research and protocols. The initial affirmation from transplantation of bulge stem cells showed that stem cells can further differentiate into interfollicular epidermis, sebaceous gland and hair follicle lineages. Further studies (Takeo et al., 2015) showed that bulge stem cells contributed well enough for the regeneration of hair follicle but not for the maintenance of the interfollicular epidermis but meanwhile when there's some sort of injury, it shifted its function mainly towards the maintenance of the interfollicular epidermis to help healing the wound.

And observations later produced more such evidences like sebaceous-gland cells are maintained by progenitors located above the bulge, which express the Blimp1 protein during morphogenesis. Studies have shown that stem cell repair induce the major mechanism of secretion of paracrine factors which enhance wound healing. Similarly like the paracrine factors, mesenchymal stem cells(MSCs), also has the ability to promote healing by activating host cells. In one study, allogeneic MSCs generated from bone marrow were injected into cutaneous wounds in mice and found to produce keratinocyte-specific proteins and contribute to the creation of glandular structures after damage. Even though long-term engraftment wasn't as fruitful, MSC-treated wounds had a higher amount of released proangiogenic factors. Local injection of allogeneic MSCs has been demonstrated in our laboratory. Taken together, these findings imply that stem cell injection advantages are due to early cytokine release rather than long-term engraftment and differentiation.

The stem cell's dynamic microenvironment, or niche, is in charge of controlling their "stem-like" activity throughout life.

Adjacent cells (both stem and non-stem cells), signalling chemicals, matrix architecture, physical forces, oxygen tension, and other environmental variables make up a niche.

Following is a better breakdown of what these niches are and how they influence cell activity (Wong et al., 2012).

Table 2. The diverse types of cell niches

The Epidermis cells niche	The Dermal niche	The Adipose niche	Engineering niche
3 major stem cells population – a) Hair follicle Bulge b) Sebaceous gland c) Interfollicular epithelium	composed of – a) heterogeneous matrix of collagens b) elastin c) glycosaminoglycans interspersed with cells of various embryonic origin.	fat cells called adipocytes. Adipocytes are energy storing cells.	To emulate these dynamic microenvironments, tissue created systems will need to be increasingly scalable, adjustable, and customizable.

<p>Epithelial stratification, hair folliculogenesis, and wound repair are all regulated by this protein.</p>	<p>This dermal unit contains at least three unique populations of progenitor cells that regulate expression of the transcription factor Sox2</p>	<p>Signalling pathways- VEGF PPARγ FGF2 MMPs PDGF</p>	<p>In order to examine perivascular stem cell niches in vitro, researchers constructed unique three-dimensional microfluidic devices.</p>
<p>Lineage tracing and gene mapping experiments have elucidated key components in epidermal homeostasis.</p>	<p>Skin-derived precursor (SKP) cells are thought to originate in part from the neural crest and have been shown to exit the dermal papilla niche and contribute to cutaneous repair.</p>	<p>Surface and structural proteins- CD29 CD44 CD73 CD90 CD105 CD166</p>	<p>Researchers have been able to create complicated three-dimensional habitats using bioengineering techniques in order to control stem cell fate.</p>
<p>Complex intraepithelial networks, signals from the dermis (e.g., periodic expression of BMP2 and BMP4) seems to regulate epithelial processes</p>	<p>perivascular sites in the dermis have been demonstrated to act as an MSC-like niche in human scalp skin.</p>	<p>harvested from human burn wounds and shown to engraft into cutaneous wounds in a rat model</p>	<p>Other researchers have discovered that oxygen tension, pH levels, and even wound electric fields can affect stem cell life, implying that the development of new sensor devices in the future will allow for even finer control of chemical microgradients within created niches.</p>
<p>Dermal stem cells have the potential to develop into functional epidermal melanocytes.</p>	<p>Fibroblasts have also been shown to preserve multilineage potential in vitro, suggesting that they may play a significant part in skin regeneration, but this has yet to be tested.</p>	<p>Multipotent cells have the potential to be used in a variety of skin-repair applications.</p>	<p>Current niche biology research has been conducted in culture systems or rodent models, with findings that will need to be rigorously verified in human tissues before being used in therapeutic settings.</p>

Further studied have demonstrated that irreversibly committed progeny from an epithelial stem cell lineage may be “recycled” and used for the regenerative niche providing evidence of complexity of epidermal regeneration.		studies indicate that the ASC niche is closely associated with follicular and vascular homeostasis but further studies may define its role in skin homeostasis	
--	--	--	--

Optics and rebirth of cells that support vision:

The two most important organs: retina and lens, located at the front and back of the eye, plays a significant role in vision. The soluble proteins like denucleated fibres and crystallins are in charge of making the lens mostly transparent. The lens also consists of epithelial cells as a monolayer in its anterior side which repeatedly undergo the process of proliferation and differentiation forming fibres near its posterior side. The lens capsule responsible for covering the lens externally, is comprised of extracellular matrix. Light travels through the lens and gets focused on the retina which further performs the function of converting light into signals (Vigneswara et al., 2015). Opsins, a group of proteins are responsible for this entire process of light conversion. Later these light signals are transferred by means of the optic nerve finally reaching the brain which results in vision. A large number of cells types like cones, Muller cells, rods, horizontal cells, ganglion cells, amacrine cells, bipolar cells and pigment epithelial cells are contained in the retina. Mammalian lens do not have the ability to regenerate.

A most common eye disease leading to human blindness can result from opacification of cataract or the lens. Now a days lens opacification is treated by cataract surgery, a process of eliminating lens fibres leaving behind the lens capsule. The left-over epithelial cells present in the capsular bag further undergo the process of regeneration and differentiation producing new fibres. Sometimes, secondary cataract maybe produced from the cataract surgery by the process of EMT which is also known as epithelial to mesenchymal transition. TGF- β , a multifunctional growth factor regulates this entire process by mediating the process of epithelial cells differentiation producing elongated myofibroblast cells which further express a smooth muscle protein. A recent study also showed that secondary cataract formation can be delayed by a C5R antagonist.

However, lens regeneration is often found in lower vertebrates like newts which have the ability to regenerate the lens both as an adult or as a frog tadpole. The iris pigmented epithelial cells present in newts at the posterior side of their eye, undergo the process of trans differentiation forming lens epithelial cells which in course of time regenerate the lens. This process is associated with Pax6, FGF, Six3, Shh, Prox1, BMP, Wnt, and retinoic acid (Dietrich, Schrader, 2020). In frog tadpoles, trans differentiating cornea eventually bring lens regeneration using several transcriptional factors like Sox3, Otx2, Pax6, and Prox1. There have also been studies showing different signalling pathways participating in the regeneration process of amphibian lens. However, no studies till date showed evidence of retina regeneration in mammals post injury. An experiment unfolds that Müller glia cells show active response to damage in mammalian models while pigmented progenitor cells is responsible for carrying out the process of trans differentiation finally generating neuronal progenitor-like cells.

FGF and Wnt, the putative proliferation pathways were modified and manipulated in some studies to make the process of retina regeneration a most effective one. The most

dominant models for the process of retina regeneration have always been pre-, post-hatch chicks, amphibians and fishes. In amphibian retina, the regeneration process occurs when the normal development of retina is recapitulated by the retina pigmented epithelium through the process of trans differentiation (Grigoryan, 2018). However, in fishes, the regeneration of retina is usually accomplished when the residual progenitor cells are differentiated into rod photoreceptors, Müller glia then undergo the process of dedifferentiation giving rise to a progenitor-like state which further led to the rods and many other neuronal cell types regeneration. There are several other sources of cells which potentially assist the process of retina regeneration in fishes. These cells are mostly found in the ciliary marginal zone and the circumferential germinal zone.

Additionally, ability to regenerate retina was also observed in embryonic chicks when treated with growth factors. The pathways which crucially takes part in this regeneration process are BMP, FGF and Shh. The Müller glia present in post-hatch chicks have been reported to possess certain ability to carry on the process of retina regeneration. A study also unveiled that in vivo stem cells like iPSC and ESC via differentiation contribute in the process of retinal regeneration finally producing retinal neurons .

Developments in the liver cell regeneration arena:

Regeneration of liver as a response to liver injury can happen in two different ways. Either by the proliferation and regeneration of hepatocytes or from the reserve progenitor cell population when the hepatocytes can no longer regenerate the liver due to senescence or arrest. The main causes of liver injuries are due to drugs, toxins, resection or acute viral diseases.

Liver regeneration is a complex phenomenon that involves several intrahepatic and extra-hepatic constituents along with a huge number of signal molecules. Various extra hepatic factors like partial hepatectomy (PH), aging, platelets, hormones etc. affects the liver regeneration. Regeneration of liver after injuries are mainly achieved by the increase in the amount of organic tissues that result from the proliferation of hepatocytes. This process is highly controlled by the metabolic needs of the liver, it stops once the liver gets its appropriate body weight ratio. The molecule and cellular mechanisms behind liver regeneration is studied mainly using the two third partial hepatectomy in rodents. Later used genetically modified moles for more specific studies. Now global gene expression proliferation gives new discretion to the studies related to the liver regeneration.

The hepatocytes have the ability to re-enter the cell cycle for mitosis which helps in the liver homeostasis. Hepatocytes also show stem cell like characteristics. The hepatocytes are activated upon partial hepatectomy or liver injury which then extend towards the central area of liver lobule and replace the injured cells. The mature hepatocytes show high replication capacity and plasticity.

In hepatocyte mediated liver regeneration process Kupffer cells, hepatic stellate cells (HSC), liver sinusoidal endothelial cells, biliary epithelial cells (BECs) and extrahepatic cells interactions takes place. Also other factors such as blood flow stress, signals, hormones, immune factors, microbiota nerves etc influences this. The initiation and termination of regeneration depends on the regulation of various proliferation and antiproliferation factors (Cherian, Kang, 2006).

Increased blood flow triggers the urokinase plasminogen activator and matrix metalloproteinase to stimulate the breaking down of the extracellular matrix. This results in the release of hepatocyte growth factors (HGF) from ECM. Lipopolysaccharides are produced by inflammatory response binds with the TLR4 Receptor on Kupffer cells causing the release of tumor necrosis factor X (TNFX) and interleukin-6 (IL-6). In addition the HSCs and liver sinusoidal endothelial cells also can produce new HGF together with the growth factor and cytokinins such as epidermal growth factor (EGF) brought by the portal vein flow, liver mitogens reaches a high concentration in the designated site. Then

the HGF binds with receptor called C-Met, while TGF- α and EGF binds to their common receptor known as EGF binds to their common receptor known as EGF receptor (EGFR). This initiates various transduction pathways in hepatocytes. IL-6 can form an excited complex with IL-6R and gp 130 causing the activation of some pathways in hepatocytes thereby regulating apoptosis inhibiting nitric oxide synthase which in turn regulates the regeneration of liver.

All these pro-proliferation substance induced the sequence formation of complex between various cyclins and cyclin dependent kinases (CDK) that induces liver regeneration. Angiogenesis-2 plays an important role. Angiogenesis-2 is down regulated in initial stages of regeneration but then upregulated at the angiogenesis phase and there by regulates the vascular endothelial growth factors that promoter angiogenesis (DeLeve, 2013).

When the volume of the regenerated liver reaches the predetermined proportion termination of the liver regeneration gets activated. TGF- β act as the most significant hepatocyte proliferation inhibitor and termination signal in liver regeneration TGF- β initiates the termination of liver regeneration by regulatory DNA synthesis of cell proliferation. This together with some other negative feedback inhibitions causes the homeostasis of liver regeneration.

Hepatic progenitor cell mediated liver regeneration:

Hepatic progenitor cells (HPCs) serves as the hepatocyte reservoir when the mature hepatocytes fails to regenerate liver due to arrest. HPCs in rodents also known as hepatic oval cells, act as the bipotent progenitor cells. Under the stimulations, the quiescent HPCs proliferates and moves from the surrounding hepatic lobules to the hepatic cords and then differentiates into either hepatocytes or BECs and finally fuse to reconstruct the hepatic lobules. Also the HPCs can be considered as the dynamic stem cells that are capable of expressing different markers based on the lack of epithelial cell type and various pathological features of injury, thus differentiating into different cells. HPCs differentiate into hepatocytes in case of severe loss of hepatocytes whereas it becomes bile duct cells when cholestasis occurs (Al-Ghamdi et al., 2020). The Notch signals play a key role in BEC differentiation.

Factors influencing Liver regeneration:

1) Fibrosis:

The viral, alcoholic and autoimmune hepatitis can induce fibrosis change. The efficiency of HOCs to differentiate into mature hepatocytes is very low in alcoholic hepatitis patients. Liver fibrosis can be a reason for impaired liver regeneration. The liver with fibrosis can activate HSCs and HPCs to promote the regeneration of liver. Various pathological factors that lead to liver fibrosis can also stimulate the institution of liver regeneration.

2) Aging:

The aging liver would cause impaired liver function and poor liver regeneration after transplantation.

3) Platelet count:

From various studies it is found that low platelet count following partial hepatectomy (PH) or live liver transplantation can lead to post operative liver dysfunction and death. However the X granules produced by the platelets contains both pro-proliferation factors and anti-proliferation growth factors which shows multiple effect of platelets on liver regeneration.

4) Neural regulation and Hormones:

There is a direct feedback relationship between the lives and the brain via the autonomic nervous system. The hepatic branches of vagus nerves in rats produce vagus signals that can induce the liver regeneration. Nerve signals also induce the release of

serotonin in enterochromaffin cells after partial hepatectomy thereby facilitating liver regeneration indirectly.

5) Bile acids:

Bile acids act as an important signal regulates in the liver regeneration process; through multiple pathways.

3. Conclusion

The paper focuses on human fascination of animals' astonishing capacity to regenerate bodily parts following injury, and scientists have been drawn to study regeneration occurrences for generations. Much of the debate here is focused on how the goal of understanding the fundamental principles underlining organismal growth is fundamentally comparable to the study of regeneration. The paper has been written with rigorous and comprehensive findings of different research paper studies following Cell Regeneration of Eyes, Skin, Bone and Cardiac tissue and Liver. In a brief, research regarding regeneration of eyes is yet to accomplish something significant for human retina but few active responses has been seen in amphibians, fishes and chickens. Meanwhile, for Regeneration of bone and cardiac, discussion concerning use of 3dbioprinting and angiogenesis has been done with observations based on effects of different growth factors. Whereas, Skin regeneration discussion is based surrounding bulge and mesenchymal stem cells showing the capacity to heal. Regarding liver, the discussion sheds light on research that's been done with respect to intra and extra hepatic cells and signals, and the potential that new global gene expression and proliferation holds. As regards to scope and future of cell regeneration, progress has been made relating to regrowth and regenerative medicine and use of forefront advanced techniques following prime understanding of the molecular and structural biology will be the elementary focus for scientists for the upcoming researches.

References

- [Adolphe, Wainwright, 2005](#) – Adolphe, C., Wainwright, B. (2005). Pathways to improving skin regeneration. *Expert Reviews in Molecular Medicine*. 7(20). DOI: <https://doi.org/10.1017/S1462399405009890>
- [Al-Ghamdi et al., 2020](#) – Al-Ghamdi, T.H., Atta, I.S., El-Refaei, M. (2020). Role of interleukin 6 in liver cell regeneration after hemi-hepatectomy, correlation with liver enzymes and flow cytometric study. *Clinical and Experimental Hepatology*. 6(1). DOI: <https://doi.org/10.5114/CEH.2020.93055>
- [Amini et al., 2012](#) – Amini, A.R., Laurencin, C.T., Nukavarapu, S.P. (2012). Bone tissue engineering: Recent advances and challenges. *Critical Reviews in Biomedical Engineering*. 40(5). DOI: <https://doi.org/10.1615/CritRevBiomedEng.v40.i5.10>
- [Ansari, 2019](#) – Ansari, M. (2019). Bone tissue regeneration: biology, strategies and interface studies. *Progress in Biomaterials*. 8(4). DOI: <https://doi.org/10.1007/s40204-019-00125-z>
- [Atabay et al., 2018](#) – Atabay, K.D., LoCascio, S.A., de Hoog, T., Reddien, P.W. (2018). Self-organization and progenitor targeting generate stable patterns in planarian regeneration. *Science*. 360(6387). DOI: <https://doi.org/10.1126/science.aap8179>
- [Blanpain, 2010](#) – Blanpain, C. (2010). Stem cells: Skin regeneration and repair. *Nature*. 464(7289). DOI: <https://doi.org/10.1038/464686a>
- [Brand et al., 2007](#) – Brand, S., Dambacher, J., Beigel, F., Zitzmann, K., Heeg, M.H.J., Weiss, T.S., Prüfer, T., Olszak, T., Steib, C.J., Storr, M., Göke, B., Diepolder, H., Bilzer, M., Thasler, W.E., Auernhammer, C.J. (2007). IL-22-mediated liver cell regeneration is abrogated by SOCS-1/3 overexpression in vitro. *American Journal of*

Physiology – Gastrointestinal and Liver Physiology. 292(4). DOI: <https://doi.org/10.1152/ajpgi.00239.2006>

[Chandika et al., 2020](#) – Chandika, P., Heo, S.Y., Kim, T. H., Oh, G.W., Kim, G.H., Kim, M.S., Jung, W.K. (2020). Recent advances in biological macromolecule based tissue-engineered composite scaffolds for cardiac tissue regeneration applications. *International Journal of Biological Macromolecules*. 164. DOI: <https://doi.org/10.1016/j.ijbiomac.2020.08.054>

[Cherian, Kang, 2006](#) – Cherian, M.G., Kang, Y.J. (2006). Metallothionein and liver cell regeneration. *Experimental Biology and Medicine*. 231(2). DOI: <https://doi.org/10.1177/153537020623100203>

[DeLeve, 2013](#) – DeLeve, L.D. (2013). Liver sinusoidal endothelial cells and liver regeneration. *Journal of Clinical Investigation*. 123(5). DOI: <https://doi.org/10.1172/JCI66025>

[Dietrich, Schrader, 2020](#) – Dietrich, J., Schrader, S. (2020). Towards Lacrimal Gland Regeneration: Current Concepts and Experimental Approaches. *Current Eye Research*. 45(3). DOI: <https://doi.org/10.1080/02713683.2019.1637438>

[Dimitriou et al., 2011](#) – Dimitriou, R., Jones, E., McGonagle, D., Giannoudis, P.V. (2011). Bone regeneration: Current concepts and future directions. *BMC Medicine*. 9. DOI: <https://doi.org/10.1186/1741-7015-9-66>

[Duelen, Sampaolesi, 2017](#) – Duelen, R., Sampaolesi, M. (2017). Stem Cell Technology in Cardiac Regeneration: A Pluripotent Stem Cell Promise. *IEBioMedicine*. 16. DOI: <https://doi.org/10.1016/j.ebiom.2017.01.029>

[Duncan et al., 2009](#) – Duncan, A.W., Dorrell, C., Grompe, M. (2009). Stem Cells and Liver Regeneration. *Gastroenterology*. 137(2). DOI: <https://doi.org/10.1053/j.gastro.2009.05.044>

[Fujita et al., 2000](#) – Fujita, M., Furukawa, H., Hattori, M., Todo, S., Ishida, Y., Nagashima, K. (2000). Sequential observation of liver cell regeneration after massive hepatic necrosis in auxiliary partial orthotopic liver transplantation. *Modern Pathology*. 13(2). DOI: <https://doi.org/10.1038/modpathol.3880029>

[Gonzalez de Torre et al., 2020](#) – Gonzalez de Torre, I., Alonso, M., Rodriguez-Cabello, J.C. (2020). Elastin-Based Materials: Promising Candidates for Cardiac Tissue Regeneration. *Frontiers in Bioengineering and Biotechnology*. 8. DOI: <https://doi.org/10.3389/fbioe.2020.00657>

[González-Sastre et al., 2012](#) – González-Sastre, A., MDolores, M., Saló, E. (2012). Inhibitory smads and bone morphogenetic protein (BMP) modulate anterior photoreceptor cell number during planarian eye regeneration. *International Journal of Developmental Biology*. 56(1–3). DOI: <https://doi.org/10.1387/ijdb.123494ag>

[Grigoryan, 2018](#) – Grigoryan, E.N. (2018). Molecular Factors of the Maintenance and Activation of the Juvenile Phenotype of Cellular Sources for Eye Tissue Regeneration. *Biochemistry (Moscow)*. 83(11). DOI: <https://doi.org/10.1134/S0006297918110032>

[Handberg-Thorsager, Saló, 2007](#) – Handberg-Thorsager, M., Saló, E. (2007). The planarian nanos-like gene Smednos is expressed in germline and eye precursor cells during development and regeneration. *Development Genes and Evolution*. 217(5). DOI: <https://doi.org/10.1007/s00427-007-0146-3>

[Huang et al., 2020](#) – Huang, X., Liu, X., Shang, Y., Qiao, F., Chen, G. (2020). Current Trends in Research on Bone Regeneration: A Bibliometric Analysis. *BioMed Research International*. DOI: <https://doi.org/10.1155/2020/8787394>

[Iaquinta et al., 2019](#) – Iaquinta, M.R., Mazzoni, E., Bononi, I., Rotondo, J.C., Mazziotta, C., Montesi, M., Sprio, S., Tampieri, A., Tognon, M., Martini, F. (2019). Adult Stem Cells for Bone Regeneration and Repair. *Frontiers in Cell and Developmental Biology*. 7. DOI: <https://doi.org/10.3389/fcell.2019.00268>

- Li et al., 2020 – Li, W., Li, L., Hui, L. (2020). Cell Plasticity in Liver Regeneration. *Trends in Cell Biology*. 30(4). DOI: <https://doi.org/10.1016/j.tcb.2020.01.007>
- Li, Hua, 2017 – Li, N., Hua, J. (2017). Immune cells in liver regeneration. *Oncotarget*. 8(2). DOI: <https://doi.org/10.18632/oncotarget.12275>
- Lin et al., 2020 – Lin, Y.H., Kang, L., Feng, W.H., Cheng, T.L., Tsai, W.C., Huang, H.T., Lee, H.C., Chen, C.H. (2020). Effects of lipids and lipoproteins on mesenchymal stem cells used in cardiac tissue regeneration. *International Journal of Molecular Sciences*. 21(13). DOI: <https://doi.org/10.3390/ijms21134770>
- LoCascio et al., 2017 – LoCascio, S.A., Lapan, S.W., Reddien, P.W. (2017). Eye Absence Does Not Regulate Planarian Stem Cells during Eye Regeneration. *Developmental Cell*. 40(4). DOI: <https://doi.org/10.1016/j.devcel.2017.02.002>
- Marolt Presen et al., 2019 – Marolt Presen, D., Traweger, A., Gimona, M., Redl, H. (2019). Mesenchymal Stromal Cell-Based Bone Regeneration Therapies: From Cell Transplantation and Tissue Engineering to Therapeutic Secretomes and Extracellular Vesicles. *Frontiers in Bioengineering and Biotechnology*. 7. DOI: <https://doi.org/10.3389/fbioe.2019.00352>
- Martin, 1997 – Martin, P. (1997). Wound healing – Aiming for perfect skin regeneration. *Science*. 276(5309). DOI: <https://doi.org/10.1126/science.276.5309.75>
- Nourian Dehkordi et al., 2019 – Nourian Dehkordi, A., Mirahmadi Babaheydari, F., Chehelgerdi, M., Raeisi Dehkordi, S. (2019). Skin tissue engineering: Wound healing based on stem-cell-based therapeutic strategies. *Stem Cell Research and Therapy*. 10(1). DOI: <https://doi.org/10.1186/s13287-019-1212-2>
- Radhakrishnan et al., 2014 – Radhakrishnan, J., Krishnan, U.M., Sethuraman, S. (2014). Hydrogel based injectable scaffolds for cardiac tissue regeneration. *Biotechnology Advances*. 32(2). DOI: <https://doi.org/10.1016/j.biotechadv.2013.12.010>
- Rebouças et al., 2016 – Rebouças, J. de S., Santos-Magalhães, N.S., Formiga, F.R. (2016). Cardiac regeneration using growth factors: Advances and challenges. *Arquivos Brasileiros de Cardiologia*. 107(3). DOI: <https://doi.org/10.5935/abc.20160097>
- Sadek, Olson, 2020 – Sadek, H., Olson, E.N. (2020). Toward the Goal of Human Heart Regeneration. *Cell Stem Cell*. 26(1). DOI: <https://doi.org/10.1016/j.stem.2019.12.004>
- Shpichka et al., 2019 – Shpichka, A., Butnaru, D., Bezrukov, E.A., Sukhanov, R.B., Atala, A., Burdukovskii, V., Zhang, Y., Timashev, P. (2019). Skin tissue regeneration for burn injury. *Stem Cell Research and Therapy*. 10(1). DOI: <https://doi.org/10.1186/s13287-019-1203-3>
- Smagul et al., 2020 – Smagul, S., Kim, Y., Smagulova, A., Raziyeva, K., Nurkesh, A., Saparov, A. (2020). Biomaterials loaded with growth factors/cytokines and stem cells for cardiac tissue regeneration. *International Journal of Molecular Sciences*. 21(17). DOI: <https://doi.org/10.3390/ijms21175952>
- So et al., 2020 – So, J., Kim, A., Lee, S. H., Shin, D. (2020). Liver progenitor cell-driven liver regeneration. *Experimental and Molecular Medicine*. 52(8). DOI: <https://doi.org/10.1038/s12276-020-0483-0>
- Takeo et al., 2015 – Takeo, M., Lee, W., Ito, M. (2015). Wound healing and skin regeneration. *Cold Spring Harbor Perspectives in Medicine*. 5(1). DOI: <https://doi.org/10.1101/cshperspect.a023267>
- Vig et al., 2017 – Vig, K., Chaudhari, A., Tripathi, S., Dixit, S., Sahu, R., Pillai, S., Dennis, V.A., Singh, S.R. (2017). Advances in skin regeneration using tissue engineering. *International Journal of Molecular Sciences*. 18(4). DOI: <https://doi.org/10.3390/ijms18040789>
- Vigneswara et al., 2015 – Vigneswara, V., Esmaili, M., Deer, L., Berry, M., Logan, A., Ahmed, Z. (2015). Eye drop delivery of pigment epithelium-derived factor-34 promotes

retinal ganglion cell neuroprotection and axon regeneration. *Molecular and Cellular Neuroscience*. 68. DOI: <https://doi.org/10.1016/j.mcn.2015.08.001>

[Wong et al., 2012](#) – Wong, V.W., Levi, B., Rajadas, J., Longaker, M.T., Gurtner, G.C. (2012). Stem cell niches for skin regeneration. *International Journal of Biomaterials*. DOI: <https://doi.org/10.1155/2012/926059>

[Xu et al., 2020](#) – Xu, G.P., Zhang, X.F., Sun, L., Chen, E.M. (2020). Current and future uses of skeletal stem cells for bone regeneration. *World Journal of Stem Cells*. 12(5). DOI: <https://doi.org/10.4252/wjsc.v12.i5.339>

[Zhai et al., 2020](#) – Zhai, M., Zhu, Y., Yang, M., Mao, C. (2020). Human Mesenchymal Stem Cell Derived Exosomes Enhance Cell-Free Bone Regeneration by Altering Their miRNAs Profiles. *Advanced Science*. 7(19). DOI: <https://doi.org/10.1002/adv.202001334>